Jessica Filipa Monteiro Martins Pereira

Degree in Biomedical Laboratory Sciences

Bacterial Pathogens Survival Strategies
The Haem Biosynthesis Pathway in *Campylobacter jejuni*

Dissertation to obtain the Master's degree in Biotechnology

Supervisor: Professor Dr Lígia Saraiva, Head of Laboratory Molecular Mechanisms of Pathogen Resistance, ITQB-NOVA

Co-supervisor: Dr Jordi Beas, Researcher at Laboratory Molecular Mechanisms of Pathogen Resistance, ITQB-NOVA

Opponent: Dr Mónica Oleastro, Head of The National Reference Laboratory for Gastrointestinal Infections, INSA

President: Professor Dr Ana Cecília Roque, Head of the Biomolecular Engineering Laboratory, FCT-UNL

December, 2020

Jessica Filipa Monteiro Martins Pereira

Degree in Biomedical Laboratory Sciences

Bacterial Pathogens Survival Strategies
The Haem Biosynthesis Pathway in *Campylobacter jejuni*

Dissertation to obtain the Master's degree in Biotechnology

Supervisor: Professor Dr Lígia Saraiva, Head of Laboratory Molecular Mechanisms of Pathogen Resistance, ITQB-NOVA

Co-supervisor: Dr Jordi Beas, Researcher at Laboratory Molecular Mechanisms of Pathogen Resistance, ITQB-NOVA

Opponent: Dr Mónica Oleastro, Head of The National Reference Laboratory for Gastrointestinal Infections, INSA

President: Professor Dr Ana Cecília Roque, Head of the Biomolecular Engineering Laboratory, FCT-UNL

December, 2020

Bacterial Pathogens Survival Strategies – The Haem Biosynthesis Pathway in *Campylobacter jejuni*

Em memória da ciência e de novas descobertas:

… “Eles não sabem, nem sonham/ Que o sonho comanda a vida/ E que sempre que um homem sonha/ O mundo pula e avança/ Como bola colorida/ Entre as mãos de uma criança” …

Gedeão, A. (1956). Poema Pedra Filosofal. *in* Movimento Perpétuo. Local: Porto Editora.

Acknowledgments

Reservo este espaço para deixar um profundo agradecimento a todos os que de certa forma contribuíram e apoiaram o desenvolvimento desta dissertação.

Em primeiro lugar, gostaria de agradecer à Dra. Lígia Saraiva, pela oportunidade que me deu para integrar a sua equipa e confiar em mim para a realização deste trabalho. Os seus ensinamentos e conselhos foram preciosos para o meu desenvolvimento laboratorial e enquanto aspirante a cientista, muito obrigada.

My sincere thanks to Jordi Beas, who led me to where I am today, passed me his passion for science and taught me with patience, from theory to practice, all his knowledge, not giving up on me. His support was essential for the writing of this thesis, thank you.

In particular, I would like to express my gratitude to the entire Molecular Mechanisms of Pathogen Resistance Lab, by team spirit and help, which allowed me never to feel helpless when everything was alien to me. So, I genuinely thank Jordi Beas, Marco Videira, Sandra Carvalho, Liliana Silva, Cláudia Freitas, Joana Batista, Sofia Mendes, Ana Oliveira, Laura Veiga and Salomé Mota, for all their support and kindness.

Aos meus fiéis companheiros da marmita, que entre incubações e centrifugações arranjavam sempre tempo para a abençoada reunião de almoço, essencial para a manutenção da nossa sanidade mental. À Catarina, à Rita, à Laura, à Jennifer, ao Gonçalo e a Salomé, obrigada.

À minha tríade de biotec, a Catarina, a Marta e a Andreia, que mesmo não estando fisicamente fizeram com que nunca me sentisse sozinha. Por isso queria agradecer-vos por todo o apoio, em todos os detalhes, e dizer que sem vocês chegar até aqui teria sido muito mais difícil, obrigada.

Queria agradecer à minha família, pelo apoio incondicional, por acreditarem em mim e no que eu própria duvidei ser capaz de fazer, por me dizerem que se orgulham e me darem a confiança necessária para continuar. Sem vocês tudo isto não seria possível, obrigada.

Ao meu namorado Pedro, que aturou os meus desesperos e angústias, ouviu discursos infindáveis sobre genética e me deu força e motivação para continuar quando estas escasseavam. Sem ele, este desafio teria sido muito mais difícil, obrigada.

Por fim, mas não menos importantes, gostaria de agradecer às minhas amigas de longa data, pelo apoio imprescindível, desde tardes infindáveis com companhia para a redação da tese até à compreensão numa fase em que nem sempre estive presente, física ou psicologicamente, obrigada meninas.

Gostaria de deixar também um agradecimento ao R&D Project PTDC/BIA-BQM/28642/2017 da FCT que financiou todo este trabalho de investigação.

Abstract

Campylobacter jejuni is one of the most common foodborne pathogens responsible for the majority of the worldwide diarrhoeal infections, causing illness to more than 137 million people every year according with World Health Organization. Despite its widespread and persistence, the essential molecular mechanisms for *C. jejuni* successful development and infection of the host are still poorly understood. This is the case of haem homeostasis, which is an essential process to bacterial development and plays a very important role during the infection process. Haem is an iron-containing porphyrin that is abundantly present in all life domains and acts as a prosthetic group for a diverse group of proteins. Haem can be either endogenously synthesised or acquired from the host. This work aims to identify and characterise *C. jejuni*'s haem biosynthesis pathway to better understand the role of haem biosynthesis in *C. jejuni*'s pathogenicity. In this work, I cloned the putative genes constituting the haem biosynthetic pathway of *C. jejuni* in plasmids designed for *E. coli* overexpression. To analyse the activity of each of the enzymes of the pathway, I complemented *E. coli*'s haem biosynthesis mutants with *C. jejuni*'s enzymes. Our results showed that *C. jejuni*'s genome encodes for a complete Protoporphyrin Dependent Pathway (PPD). It was further confirmed that UroD and PpfC enzymes possessed uroporphyrinogen decarboxylase and protoporphyrin ferrochelatase activities, respectively. Overall, our results strongly suggest that *C. jejuni* encode for a full functional PPD haem biosynthesis pathway. Further work should aim at the study of the role of these proteins in *C. jejuni*'s infection development.

Keywords: *Campylobacter jejuni*; haem biosynthesis Gram negatives; haem in Gram negative

Resumo

Campylobacter jejuni é um dos agentes patogénicos alimentares mais comuns, responsáveis pela maioria das infeções diarreicas a nível mundial, causando doença a mais de 137 milhões de pessoas por ano, de acordo com dados da Organização Mundial da Saúde. Apesar da sua difusão e persistência neste tipo de infeção, os mecanismos moleculares essenciais para o sucesso do seu desenvolvimento e infeção no hospedeiro ainda não são completamente compreendidos. É o caso da homeostase do hemo, que é um processo essencial para o desenvolvimento bacteriano e desempenha um papel muito importante no processo de infeção. O hemo é uma porfirina contendo ferro que está fortemente presente em todos os domínios da vida e atua como um grupo prostético para um variado grupo de proteínas. O hemo pode ser sintetizado de forma endógena ou adquirido no hospedeiro. Este trabalho visa identificar e caracterizar a via de biossíntese do hemo em *C. jejuni* para melhor compreender o papel desta porfirina na patogenicidade de *C. jejuni*. Neste trabalho, clonei os genes putativos que constituem a via hemossintética de *C. jejuni* em plasmídeos concebidos para testes de sobreexpressão em *E. coli*. Para analisar a atividade de cada uma das enzimas nesta via, complementei mutantes da biossíntese de hemo de *E. coli* com enzimas de *C. jejuni*. Os nossos resultados mostraram que o genoma de *C. jejuni* codifica uma Via Dependente de Protoporfirina (PPD). Confirmamos ainda que as enzimas UroD e PpfC possuíam atividades de uroporfirinogénio decarboxilase e protoporfirina ferroquelatase, respectivamente. No geral, os nossos resultados fortemente sugerem que *C. jejuni* codifica para uma via dependente de porfirina, completa e funcional, para biossíntese de hemo. Futuros trabalhos devem visar o estudo do papel destas proteínas no desenvolvimento de infeção de *C. jejuni*.

Palavras-chave: *Campylobacter jejuni*; Biossíntese de hemo em bactérias Gram negativas; Hemo em Gram negativos

Table of Content

Index of Figures

Index of Tables

List of Abbreviations

ALA 5-Aminolevulinic acid

ALAS 5-Aminolevulinic acid synthase

Ahb Alternative haem biosynthesis Pathway

Amp Ampicillin

CDT Cytolethal distending toxin

CDC2 Cyclin-dependent kinase 2

CgoX Coproporphyrinogen oxidase

CgdC Coproporphyrinogen III oxidase

CgdH Coproporphyrinogen III dehydrogenase

ChdC Coprohaem decarboxylase

Cje *Campylobacter jejuni*

CoA Succinyl coenzyme A

Coprohaem Fe-coproporphyrin III

CPD Coproporphyrin-dependent branch

CpfC Coproporphyrin ferrochelatase

gDNA Genomic DNA

FP French Press

GluS Glutamyl-synthase

He Haemin

Hem$^-$ Haemin deficient

HmbS Hydroxymethylbilane synthase

Hmb Hydroxymethylbilane

Hepes Zwitterionic sulfonic acid buffering agent

Kan Kanamycin

MM Milimolar

MQ MillliQ®

µg Micrograms

µL Microlitter

Ng Nanograms

Pbg Porphobilinogen

PbgS Porphobilinogen synthase

PCR Polymerase Chain Reaction

PgdH1 Protoporphyrinogen IX desidrogenase 1

PgdH2 Protoporphyrinogen IX desidrogenase

PgoX Protoporphyrinogen IX oxidase

Pmol Picomol

PpfC Protoporphyrin ferrochelatase

PPD Protoporphyrin-dependent branch

PROTO'GEN IX Protoporphyrinogen IX

SDS-PAGE Sodium dodecyl sulfate-polyacrylamide gel

SirA Uroporphyrinogen III methyltransferase

SirB Sirohydrochlorin ferrochelatase

SirC Dihydrochlorin dehydrogenase

SAM *S*-adenosyl-$_L$-methionine

TMBZ Tetramethylbenzidine

U Units

URO'GEN III Uroporphorinogen III

UroS Uroporphyrinogen synthase

UroD Uroporphyrinogen decarboxylase

WHO World Health Organization

Chemical formulas

NH_4Cl Ammonium chloride

CO_2 Carbon Dioxide

$CaCl_2$ Calcium Chloride

DMSO Dimethyl sulfoxide

$Na_2HPO_4.7H_2O$ Di-sodium hydrogen phosphate heptahydrate

Fe^{2+} Ferrous iron

4Fe-4S Iron sulfur cluster

N_2 Nitrogen

NO_2 Nitrite

NO_3 Nitrate

$MgSO_4.7H_2O$ Magnesium sulfate heptahydrate

KH_2PO_4 Potassium phosphate monobasic

O_2 Oxygen

KH_2PO_4 Potassium phosphate monobasic

$MnCl_2.4H_2O$ Manganese(II) chloride tetrahydrate

NaCl Sodium chloride

$NaHPO_4.2H_2O$ Sodium phosphate dibasic dihydrate

NaOH Sodium hidroxide

$NaNO_3$ Sodium nitrate

$NaNO_2$ Sodium nitrite

H_2O Water

1

Introduction

Campylobacter jejuni is one of the most common foodborne pathogens causing the largest part of gastroenteritis illness worldwide, affecting more than 137 million people every year, according to World Health Organization (WHO, 2020). Although its presence is persistent in this type of infection, its pathogenicity and molecular biology are not yet well-known. *Campylobacter jejuni* is a commensal microorganism of many avian species and mammals. In humans, *C. jejuni* is mostly acquired by contact with infected poultry, by mishandling or consumption of unwell cooked meat and less frequently by contaminated dairy products (Figure 1.1) (Allos, 2001; Altekruse *et al*., 1999; Bolton, 2015; Young, Davis, & Dirita, 2007).

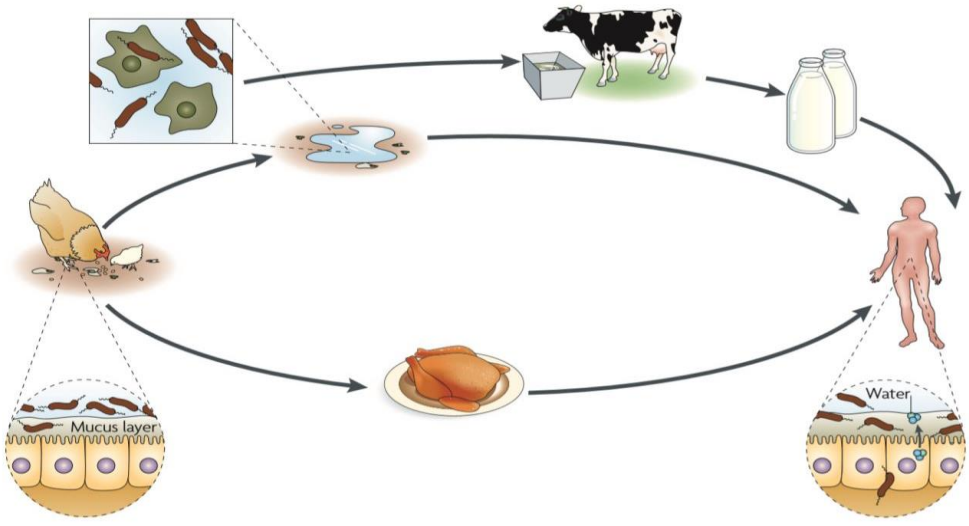

Figure 1.1 - Sources of transmission of *Campylobacter jejuni* to humans. The infection is acquired by the consumption of poultry, dairy products, or contaminated water. After colonisation, the pathogen adheres and invades the host epithelium, where it produces toxins that promote its persistence and survival. (Young *et al*., 2007)

1. I Bacterial features

Campylobacter jejuni is a helical-shaped flagellated Gram-negative bacterium. This enteric pathogen belongs to the class of epsilon proteobacteria. The optimal environment for the growth of this organism in the laboratory is a mimic of gut conditions, such as microaerobic conditions (low amounts of O_2 and high amounts of CO_2 and N_2 concentrations) and temperature between 37ºC and 42ºC (Allos, 2001; Altekruse *et al*., 1999).

In 2000, the full sequencing of *Campylobacter jejuni* NCTC11168 strain was achieved the by Sanger Center, revealing that *C. jejuni* has a circular chromosome with 1,641,481 base pairs encoding 1654 proteins. The studies showed that this bacterium presents hypervariable regions that might be involved in survival to environmental adversities (Parkhill, Wren, Mungall, Ketley, & Churcher, 2000).

1. II Bacterial pathogenicity

After *Campylobacter jejuni* ingestion, symptoms develop from two to five days and infection usually lasts 7 days. The infection affects the gastrointestinal tract and the illness is mostly characterised by symptoms that can go from mild diarrhea up to an inflammatory diarrhoea (watery and bloody), abdominal cramps, and fever (Bolton, 2015). The symptoms can last for weeks until total excretion from the organism, depending on the immune competence of the host. The gastrointestinal colonisation may give rise to inflammation of the gallbladder, pancreas, peritoneum, and even a substantial haemorrhagic infection. Less often, it can cause non-intestinal infections like meningitis, osteoarthritis, septic arthritis, or bacteraemia. In extreme cases of prolonged infection, campylobacteriosis can lead to Guillain-Barré syndrome and Miller-Fisher syndrome that are severe immune-mediated nerve damage illnesses that can cause acute neuroparalysis (Allos, 2001; Ang, 2001; Wassenaar, 1997).

As mentioned before, poultry is the major source of transmission to humans and the primary reservoir of *C. jejuni*. It colonises the caecal mucosa of the animal and does not cause illness. After avian gut colonisation, the bacteria are transmitted to humans. The infected poultry or dairy products are ingested and moves from the stomach to the intestine tract. It settles in the small intestine where invades and proliferates the human epithelium, until passes to the outside through faeces (Figure 1.1)(Bolton, 2015; Young *et al*., 2007). In the infection cycle, the microorganism passes through a stressful environment as the acidic conditions of the stomach, temperature and nutrient apport variations, lower concentrations of iron, oxidative and nitrosative stress (Sarvan, Yeung, & Stintzi, 2019). For that reason, when the pathogen colonises humans, has enhanced virulence and ability to multiply comparing to that primary poultry host (Bolton, 2015). The pathogenicity of *C. jejuni* is mostly characterized by four virulence factors: motility, adherence, invasion, and toxins releasing (Bolton, 2015; Ridley, Rock, Li, & Ketley, 2006).

The motility in *C. jejuni* plays a very important role in the infection process since it has a decisive impact on bacteria adherence and penetration into the host intestinal epithelium. Therefore, flagella and bacterial shape are special elements for these bacteria successful spread assisting the passage through viscous components. Adherence is also a crucial factor for bacterial colonization, the bacteria produce specific surface proteins, called adhesins, that bind to fibronectin of the gastrointestinal epithelial cells helping in this process. Furthermore, is thought that the flagella play another essential role during the invasion step. It has a flagellar secretion mechanism that improves invasion and infection. It is also thought that the bacteria produce non-flagellar proteins and export them through the flagella to the cytoplasm of the host cells. These proteins might contribute to regulate the invasion and intracellular survival in host cells. In the host cells, *C. jejuni* synthesises several distinct cytotoxins, like haemolysins and phospholipases, that cause membrane damage and intracellular injury (Bolton, 2015; Walker *et al*., 1986). The most studied toxin is the cytolethal distending toxin (CDT) that can bind the host cell's membrane and releases an enzymatically active subunit that enters the nucleus and blocks CDC2, a kinase essential to transition from G2 phase into mitosis of the cell cycle. This can lead to nuclear deterioration and cell death. The production of this strong toxic compounds induces the diarrheal symptoms in the host (Purdy *et al*., 2000).

Besides the virulence factors that guarantee a successful spread and bacterial colonisation, the microorganisms must ensure their persistence and survival in the host environment. To this end, they must satisfy all the essential nutrients for pathogen survival and growth. These essential nutrients include macronutrients that microorganisms consume in large amounts, such as Carbon (C), Nitrogen (N), Oxygen (O), Hydrogen (H), Sulfur (S) and Phosphorus (P), as well as micronutrients that are required in small amounts, like sodium (Na), potassium (K), calcium (Ca), magnesium (Mg) and iron (Fe) (Duncan & Horan, 2003).

This work addressed the study of haem, that is an iron-containing protein cofactor. The focus of the study will be the biosynthetic production of haem in *C. jejuni*, which is an essential cofactor for pathogen development.

1. III Haem

Haem is an iron-containing porphyrin that is necessary to all organisms. Haem is a metalled tetrapyrrole as other molecules, including, bilins, corrins, chlorins, cofactor F_{430}, sirohaem, haem *b*, chlorophylls, and bacteriochlorophylls (Figure 1.2). Haem operates as a prosthetic group for proteins, such as sensor proteins, peroxidases, catalases, and cytochromes, therefore contributing to several essential biological processes involved in pathogens' invasion and survival. Haem is also important in many organisms as an iron source after being enzymatically degraded by enzyme haem oxygenase. The

synthesis of haem is done via *de novo* synthesis that enables the production of biological tetrapyrroles from simpler molecules. (Dailey *et al*., 2017).

As mentioned before, these biological tetrapyrroles are crucial to the organisms and in that way, organisms have a system to acquire haem either by their synthesis or from the host.

Haem biosynthesis in prokaryotes

Prokaryotes have mechanisms to synthesise their haem when uptake from a host is not possible. These mechanisms include three different pathways to produce haem. Each pathway share common steps to synthesise Uroporphorinogen III (URO'GEN III), an main intermediate to tetrapyrroles (Dailey *et al*., 2017).

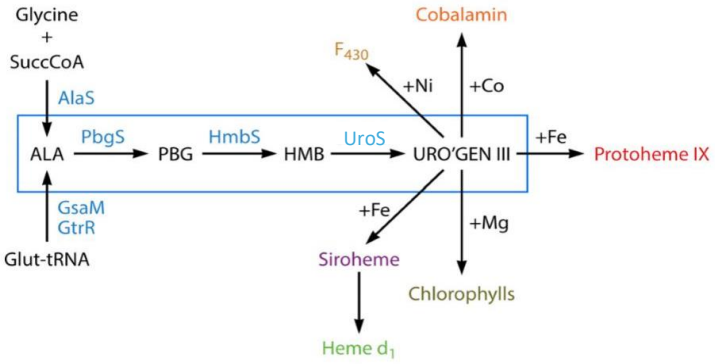

Figure 1.2 - Haem formation in prokaryotic organisms. The blue box highlights the common core to haem synthesis (Adapted from Dailey *et al*. 2017).

In this next section will be described the different steps that lead to haem biosynthesis.

Common core

The common core initiates with an intermediate, 5-Aminolevulinic acid (ALA) and can be synthesized in two different ways. The first one is called the "Shemin" or C4 pathway and is characteristic in fungi, mammals, and α-proteobacteria. In this pathway, ALA is formed by the combination of a glycine with succinyl coenzyme A (CoA), catalysed by 5-Aminolevulinic acid synthase (AlaS). The other one is designated C5 pathway, since ALA derives from C5 skeleton of tRNA-bound glutamate metabolized by glutamyl- synthase (GluS) (Figure 1.2). Generally, this last pathway is usually found in plants, archaea, and most bacteria, including prokaryotes (Dailey *et al*., 2017; Layer *et al*., 2010; Panek & Brian, 2002).

ALA is the building block of haem and the next phase includes the formation of URO'GEN III from ALA, the core route to most biological tetrapyrroles (Figure 1.2). This pathway involves three

enzymatic steps. The first enzyme, porphobilinogen synthase (PbgS), catalyses two ALA molecules to condense asymmetrically and generate a monopyrrole, the porphobilinogen (PBG). This monopyrrole is deaminated and polymerised to be transformed in URO'GEN III. Hydroxymethylbilane synthase (HmbS) deaminates PBG and promotes the assembly of four PBG leading to the synthesis of the first tetrapyrrole, the hydroxymethylbilane (HMB). Finally, uroporphyrinogen synthase (UroS) specifically cyclize HMB, conducting URO'GEN III formation (Figure 1.3) (Celis & Dubois, 2019; Dailey *et al*., 2017; Layer *et al*., 2010; Panek & Brian, 2002).

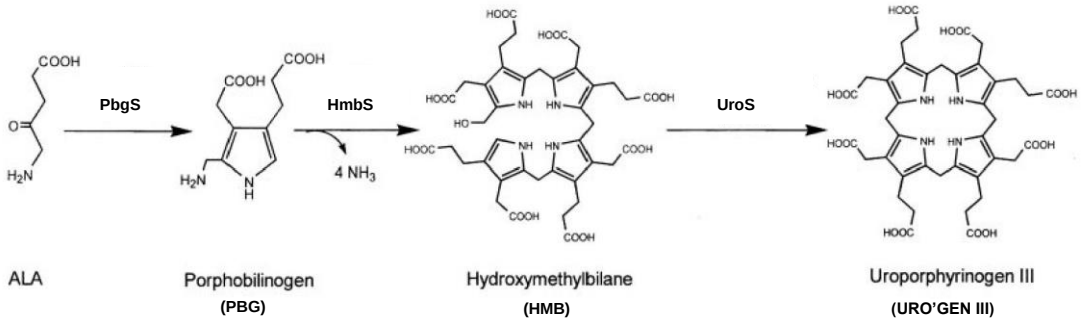

Figure 1.3 - Core pathway of tetrapyrroles formation (Adapted from Panek and Brian 2002).

So far, three different ways for haem synthesis have been established: the Protoporphyrin-dependent branch (PPD), the Coproporphyrin-dependent branch (CPD), and the Sirohaem dependent branch. These biosynthetic pathways all require the precursor URO'GEN III.

Unlike Sirohaem dependent Branch, the other two pathways, CPD and PPD, start with the decarboxylation of URO'GEN III mediated by the enzyme uroporphyrinogen decarboxylase (UroD), which leads to the formation of a common intermediate, the Coproporphyrinogen III (Figure 1.4) (Dailey *et al*., 2017; Lobo *et al*., 2015).

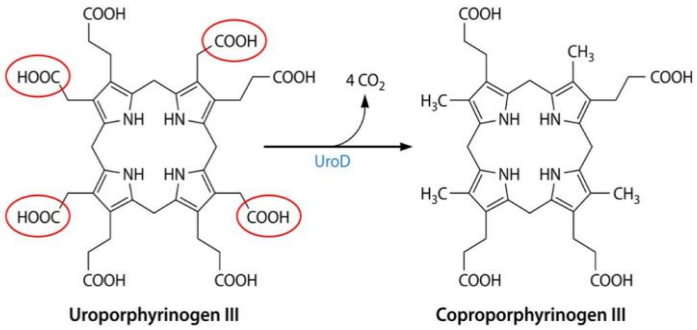

Figure 1.4 – URO'GEN III decarboxylation to form Coproporphyrinogen III (Adapted from Dailey *et al.* 2017).

In the Sirohaem dependent branch, URO'GEN III goes by several processes that involve methylation, redox reactions and metal insertion to be transformed in Sirohaem (Figure 1.5) (Bali *et al*. 2011).

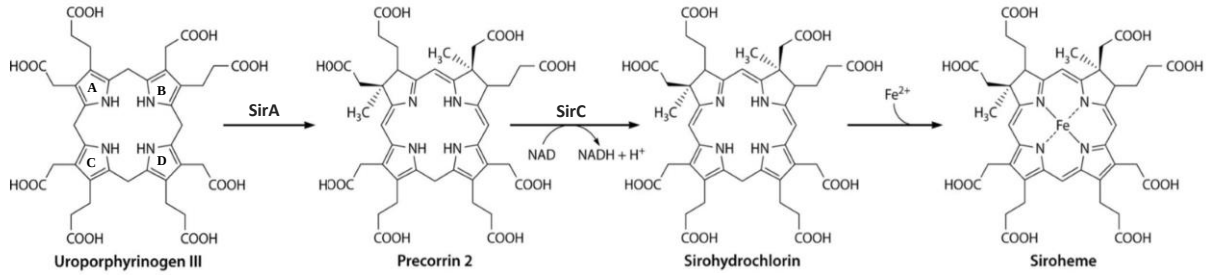

Figure 1.5 - Sirohaem formation (Adapted from Dailey *et al.* 2017).

Sirohaem dependent Branch or Alternative Pathway

The haem synthesis Sirohaem-dependent branch was discovered as an alternative pathway to the PPD or classical pathway for haem formation, also receiving the designation of Alternative haem biosynthesis (Ahb) pathway. Sirohaem is required by archaebacteria and sulfate-reducing bacteria, using it on the sulphite and nitrite reductases enzymes. These bacteria also use this pathway to produce haem (Dailey *et al*., 2017; Lobo *et al*., 2015).

Sirohaem biosynthesis vary depending on the organisms. In *Bacillus megaterium*, sirohaem formation involves three enzymatic reactions that include two methylation steps, an oxidation step and ferrochelation. The two methylation steps are coordinated by uroporphyrinogen III methyltransferase (SirA), that uses *S*-adenosyl-L-methionine (SAM) as a methyl donor to transfer two methyl groups. The first methylation occurs in rings A and B of URO'GEN III, mediated by SirA to form percorrin-1. SirA acts also in the second methylation transforming percorrin-1 into percorrin-2. Dihydrochlorin dehydrogenase (SirC) promotes an oxidation to percorrin-2 producing sirohydrochlorin. Sirohydrochlorin ferrochelatase (SirB) promotes the insertion of a Fe^{2+} into sirohydrochlorin to form sirohaem (Dailey *et al*., 2017; Tripathy *et al*., 2010; M. A. M. Videira, Lobo, Sousa, & Saraiva, 2019) (Figure 1.5). In yeast, such as *Saccharomyces cerevisiae*, the first conversion is catalysed by an enzyme called Met1p. A bifunctional enzyme, known as Met8p, performs the further dehydrogenation and ferrochelation reactions to make sirohaem (Stroupe, Leech, Daniels, Warren, & Getzoff, 2003; Tripathy *et al*., 2010; M. A. M. Videira *et al*., 2019). Some organisms, like *E. coli* and *S. enterica serovar typhimurium*, have a multifunctional enzyme called CysG. This enzyme is capable to perform all these enzymatic reactions to synthesise sirohaem (Dailey *et al*., 2017; Tripathy *et al*., 2010).

Sirohaem conversion to haem is mediated by AhbA-D enzymes. Sirohaem is decarboxylated in C12 and C18 acetic acid chains by AhbA and AhbB proteins giving rise to didecarboxysirohaem. This decarboxylated compound loses the acetic acid side chains at C2 and C7, in a SAM-dependent reaction, mediated by AhbC to form Fe-coproporphyrin III (coprohaem). Finally, another radical SAM enzyme, AhbD, stimulates the conversion of propionate side chains in C3 and C8 of coprohaem into vinyl groups to create haem (Bali *et al*., 2011; Lobo *et al*., 2014, 2015)(Figure 1.6).

Coproporphyrin-Dependent Branch (CPD) or Transitional Pathway

This pathway is used by several Gram-positive bacteria and it was the most recently discovered way to form haem (Dailey *et al*., 2017; M. Videira, Lobo, & Saraiva, 2018). Is also known as the transitional pathway since it is thought that these type of bacteria suffered an evolutionary transition between Ahb and PPD (Lobo *et al*., 2015).

As shown in Figure 1.4, Uroporphyrinogen III decarboxylation leads to Coproporphyrinogen III. In the CPD pathway, organisms oxidise the intermediate Coproporphyrinogen III into Coproporphyrin III by the action of Coproporphyrinogen oxidase (CgoX). Coproporphyrin ferrochelatase (CpfC) introduces a ferrous iron (Fe^{2+}) in coproporphyrin III to generate Fe-coproporphyrin III (coprohaem). This last one is the substrate to coprohaem decarboxylase (ChdC) that by decarboxylation give the final product, protohaem (Figure 1.6) (Dailey *et al*., 2017; Lobo *et al*., 2015).

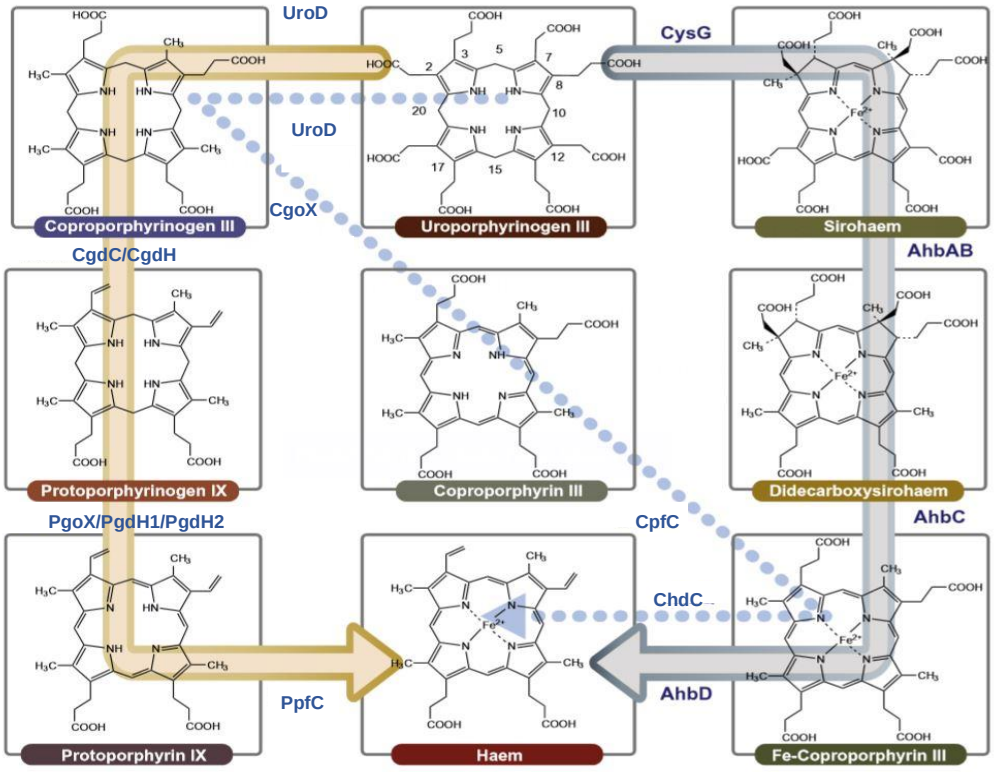

Figure 1.6 - The three different pathways and the enzymes that involve them. Yellow arrow represents PPD or Classic pathway; Blue arrow characterizes CPD or Alternative pathway; Grey arrow highlights Sirohaem pathway (Adapted from Lobo *et al.* 2015).

Protoporphyrin-Dependent Branch (PPD) or Classic Pathway

This pathway was the first one to be discovered and for that reason is also known as Classic Pathway. PPD is generally used by eukaryotes and by Gram-negative bacteria (Dailey *et al*., 2017).

In this route, the first step includes the conversion of Uroporphyrinogen III to Coproporphyrinogen III. This intermediate is transformed into Protoporphyrinogen IX and the reaction requires a decarboxylation of the propionate side chains. This reaction can be catalysed by two different enzymes, coproporphyrinogen III oxidase (CgdC) or coproporphyrinogen III dehydrogenase (CgdH). CgdC uses molecular oxygen as an electron acceptor to perform the decarboxylation, releasing H_2O_2 and CO_2 as the resulting products of the reaction. The second enzyme, CgdH, belongs to the radical SAM protein family and has an iron sulfur cluster [4Fe-4S] coordinated by three cysteines of a CX_3CX_2C motif (Dailey *et al*., 2017). The mechanism that this enzyme uses to transform the substrate into PROTO'GEN IX is completely different. This reaction does not need molecular oxygen. Instead, the electron transfer between the iron-sulfur clusters and the SAM molecules will trigger the initiation of the decarboxylation reaction of the propionate chains and will be concluded with the electron transfer to a yet unidentified electron acceptor to give Protoporphyrinogen IX and release CO_2 (Dailey *et al*., 2017).

For that conversion, an oxidative decarboxylation is required. For oxygen-dependent reactions, CgdC aids the decarboxylation using O_2 as a final electron acceptor to produce Protoporphyrinogen IX (Dailey *et al*., 2017; Layer *et al*., 2010). On the other hand, when O_2 is absent, CgdH is the enzyme that catalyses the decarboxylation. The reaction involves the electron transfer from [4Fe-4S] to a SAM molecule that enables a biocatalytic modification to do oxidative decarboxylation on Coproporphyrinogen III to form Protoporphyrinogen IX, without the oxygen requirement (Dailey *et al*., 2017; Layer *et al*., 2010).

In the next step, molecular oxygen is not required as an electron acceptor and Protoporphyrinogen IX desidrogenase 1 (PgdH1) takes the lead to oxidise Protoporphyrinogen IX to Protoporphyrin IX.

Alternatively, another enzyme, Protoporphyrinogen IX desidrogenase 2 (PgdH2), can catalyse the previous reaction. Finally, a third uncommon enzyme, can occur in a few prokaryotes for this reaction. Protoporphyrinogen IX oxidase (PgoX) is responsible for the aerobic oxidation of Protoporphyrinogen IX into Protoporphyrin IX (Dailey *et al*., 2017).

The last step includes the insertion of a Fe^{2+} molecule into the Protoporphyrin IX. This reaction is catalysed by the protoporphyrin ferrochelatase (PpfC) leading to the final product, protohaem (Dailey *et al*., 2017; Layer *et al*., 2010).

Haem in *Escherichia coli*

Escherichia coli is a Gram-negative bacterium, a facultative anaerobe and common resident of human gut. *E. coli* synthesises haem through the PPD pathway. The enzymes identified for haem biosynthesis in *E. coli* are UroD, CgdC, CgdH, PgdH1 and PpfC (Figure 1.7) (Mancini & Imlay, 2015; Zhang, Kang, Chen, & Du, 2015).

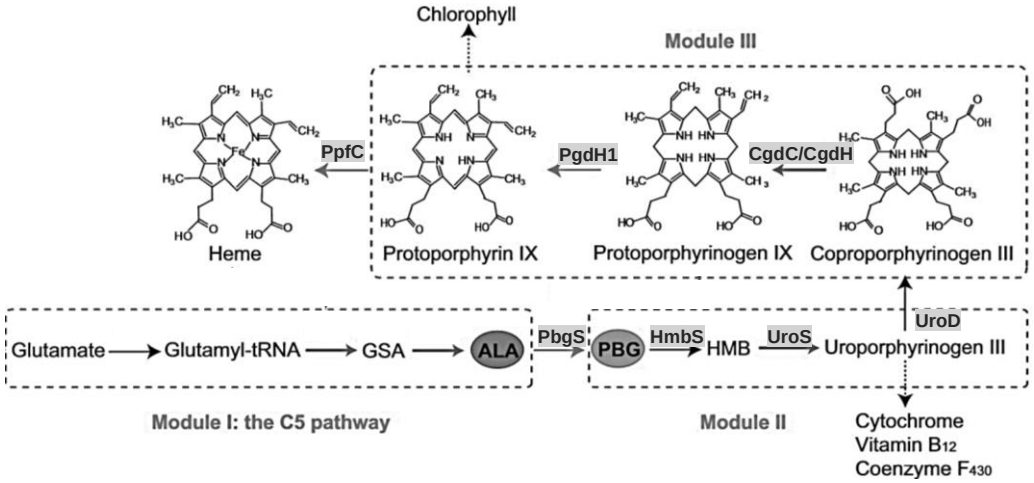

Figure 1.7 – *E. coli* haem biosynthesis by PPD pathway (Adapted from Zhang *et al.* 2015).

Most of the *E. coli* haem biosynthesis mutants have well described phenotypic characteristics. The Δ*uroD (hemE) and* Δ*pgdH1 (before called hemG)* strains, show a growth defect (dwarf colonies) when cultured in media supplemented with glucose, besides accumulation of porphyrin intermediates (Sasarman *et al*., 1979, 1975). Moreover, the Δ*ppfC* (previous *visA* or *hemH*) strain is in addition to the dwarf colony phenotype and accumulation of protoporphyrin IX, a photosensitive strain (Nakahigashi *et al.* 1991).

On the other hand, different phenotypes have been described for the Δ*cgdH* (*hemN)* strain, the first one was described in 1997, and reported that the mutant, when under anaerobic conditions, is deficient in the five type c-cytochromes production, showing also reduced nitrite reductase activity and accumulation of coproporphyrin III (Tyson, Metheringham, Griffiths, & Cole, 1997). More recently, an accumulation of coproporphyrin III was described in this mutant when under oxygen privation (Ji *et al*., 2019).

In this project, the enzymes of *Campylobacter jejuni* will be used to reconstruct step-by-step the haem biosynthesis process. To do that, one strategy would include *E. coli* mutants that are compatible in the potentially active pathway (since *E. coli* genes to synthesise haem are similar to the genes in *C. jejuni*). *E. coli* is also convenient to use due to the availability of haemin deficient (hem^-) mutants, which will allow to test *C. jejuni* genes products by complementation assays.

Furthermore, *Escherichia coli* is a commonly used organism for genetic engineering in molecular biology analysis due to its genetic flexibility, extensive characterisation, fast growth, and versatile culture conditions. *Escherichia coli* laboratory strains, such as K-12, are also considered innocuous and safer to human manipulation (Pontrelli *et al*., 2018).

1. IV Aim

The main goal of this thesis is to unveil the haem biosynthesis pathway in *Campylobacter jejuni*. Using bioinformatic tools, a putative pathway for haem biosynthesis in this microorganism was predicted. The study includes the establishment of genes involved in the pathway from URO'GEN III to haem formation. The methodology will be focused on plasmid constructions to be used in complementation assays.

2

Materials and methods

2. I. Bacterial strains and growth conditions

In the present work, the bacterial strains used were the wild type *E. coli* BW25113, the *E. coli* hem$^-$ K-12 mutants Δ*uroD* IH81, Δ*cgdH* JW3838, Δ*pgdH1* IH79 and Δ*ppfC* IH71 from Keio collection and IH *E. coli* Mutant Collection (Center, 2006; National Institute of Genetics, Microbial Physiology Laboratory, 2012). All strains used in this work are listed in Table 2.1. and the stocks were stored at -80ºC in LB liquid medium (75%) and glycerol (25%).

Table 2.1 - Strains used in this work.

Strain	Genotype	Reference
BW25113	F-, Δ*(araD-araB)567*, Δ*lacZ4787*(::rrnB-3), λ^-, *rph-1*, Δ*(rhaD-rhaB)568*, *hsdR514*	Coli Genetic Stock Center
IH81	W3110 *hemE*	Coli Genetic Stock Center
JW3838	F-, Δ*(araD-araB)567*, Δ*lacZ4787*(::rrnB-3), λ^-, *rph-1*, Δ*hemN728::kan*, Δ*(rhaD-rhaB)568*, *hsdR514*	Coli Genetic Stock Center
IH79	W3110 *hemG*	Coli Genetic Stock Center
IH71	Δ*visA*(=Δ*hemH*) HfrC lac_{am125} trp_{am} su^O	Coli Genetic Stock Center

E. coli strains were grown in LB Broth Luria-Miller rich medium (*Carl Roth* ®), if not specified otherwise (Table 2.2). LB-agar plates were prepared with the previous LB broth and supplemented with agar 1.5% for growth in solid medium.

Table 2.2 - Composition of LB Broth Luria-Miller rich medium.

Compound	Concentration (g/L)
NaCl	10
Tryptone	10
Yeast extract	5

The cultures were grown in flasks filled at 10% of its volume, for better O_2 distribution, and at 37ºC and 150 rpm. When required, growth medium was supplemented with antibiotics or other supplements. The list of supplements and antibiotics used are listed in Tables 2.3 and 2.4.

Table 2.3 - List of supplements and antibiotics used in LB media.

Supplement/Antibiotic	Final concentration	Brand	Solvent
Haemin**	10µM	*Sigma* ®	DMSO
Ampicillin Sodium Salt*	100µg/mL	*Carl Roth* ®	ddH_2O
Kanamycin Sulphate*	30µg/mL	*Carl Roth* ®	ddH_2O
Chloramphenicol*	25µg/mL	*Carl Roth* ®	Ethanol

* Filtration with 0.22µm PES membrane; ** Filtration with 0.22µm DMSO membrane

The M9 minimal medium was used for anaerobic assays with different carbon sources and electron acceptors (Table 2.4).

Table 2.4 - M9 minimal medium composition and list of supplements added.

M9 minimal medium composition	Concentration	Brand
M9 salt solution 1x*		
➢ **Di-sodium hydrogen phosphate heptahydrate ($Na_2HPO_4.7H_20$)**	➢ 7.0g/L	*Carl Roth®*
➢ **Monopotassium phosphate (KH_2PO_4)**	➢ 3.0g/L	*Merck®*
➢ **Sodium Chloride (NaCl)**	➢ 0.5g/L	*Carl Roth®*
➢ **Ammonium chloride (NH_4Cl)**	➢ 1.0g/L	*Merck®*
Magnesium sulfate heptahydrate ($MgSO_4.7H_2O$)	1mM	*Merck®*
Calcium Chloride ($CaCl_2$)	0.1mM	*Merck®*
Supplements		
Sodium Nitrite ($NaNO_2$)	2.5 mM	*Merck®*
Glycerol	0.4% (v/v)	*Merck®*
Thiamin hydrochloride	1µg/mL	*Merck®*
Sodium Fumarate	40mM	*Alfa Aesar®*
Tetramethylbenzidine (TMAO)	20mM	*TCI®*
Sodium Nitrate ($NaNO_3$)	2.5 mM	*Merck®*
Glucose	0.2%(v/v)	*Merck®*
Molybdate	10mM	-
Selenate	10mM	-
Bacto ™ Casaminoacids	0.2% (v/v)	*Sigma-Aldrich®*

* pH adjusted to 7.2 with NaOH and media sterilised

2. II. Plasmid constructions

To isolate *C. jejuni* NCTC 11168 genomic DNA, the NZY Microbial gDNA Isolation kit was used. The desired genes were amplified with specific primers and restriction sites, using this gDNA as template. After amplification, PCR amplification products and plasmids were digested to insert the DNA, and finally the fragments were ligated and transformed into the *E. coli* competent cells.

PCR amplification

The target genes amplified were *uroD*, *ppfC*, *cgdH*, and *pgdH2* from *C. jejuni*. The PCR reaction was performed as indicated in Table 2.5 and 2.6 (Appendix 6.1).

Table 2.5 - PCR mixture for one reaction.

Compound	Final concentration (1x)	Brand
Phusion Buffer HF	1x	*Thermo Scientific™*
Primer Forward	10 µM	*STAB VIDA®*
Primer Reverse	10 µM	*STAB VIDA®*
dNTPs mix	200 µM each dNTP	*Promega®*
Template gDNA	0.38ng/µL	-
Phusion High-Fidelity DNA Polymerase	2U/µL	*Thermo Scientific™*
MilliQ H_2O	Excipient qs.	-

The mixture was added in PCR tubes and placed into the thermocycler with the respective program (Table 2.6).

Table 2.6 – PCR standard program for Phusion High-Fidelity DNA Polymerase.

Cycle step	Temperature	Time	Number of cycles
Initial denaturation	98ºC	30 sec	30x**
Denaturation	98ºC	30 sec	
Annealing*	-	30 sec	
Extension	72ºC	30sec/kb	
Final extension	72ºC	7 sec	
	4ºC	∞	

*Annealing temperatures and times depend on primer's time of melting (T_m) values that are set in Appendix 1.

** To test the primers Tm the PCR program used had 34 cycles.

The PCR products were loaded in an agarose gel (1%) and fragments were purified, after checking the correct sizes, using the QIAquick® PCR purification. DNA quantification was done with *NanoDrop ™ 2000/2000c* spectrophotometer and the PCR products were stored at -20ºC.

Plasmids for cloning

The plasmids used for cloning the PCR products were pPr-IBA1 and pPr-IBA2 (Figure 2.1). The plasmid extraction from the bacterial cells was performed using a QIAprep® Spin Miniprep Kit.

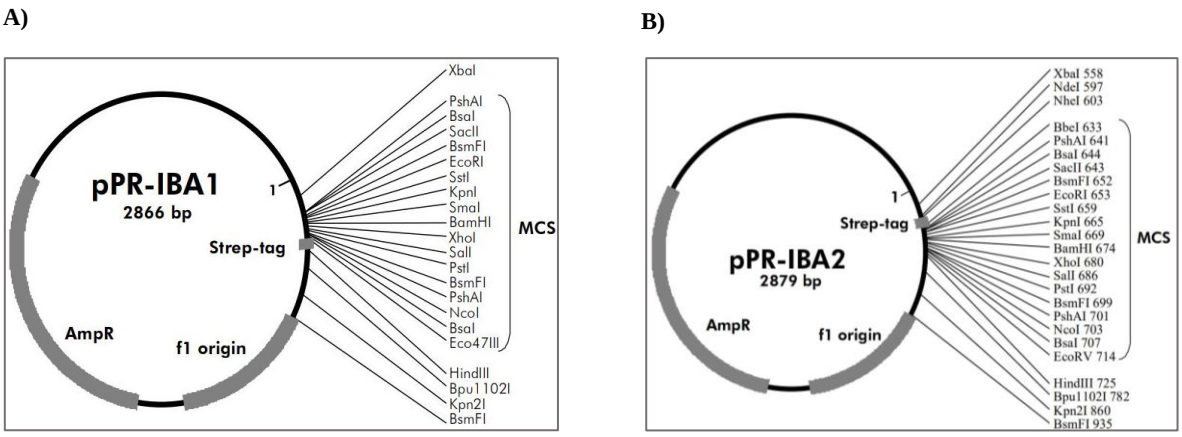

Figure 2.1 - Map of the PR-IBA1 (A) and PR-IBA 2 (B) plasmids. The replication origin, amplicillin resistance cassete (AmpR) and a multicloning site (MCS) are features represented in both plasmids.

Only pPr-IBA2 plasmid was used in the experiments of this thesis.

Enzymatic digestion

The plasmid and the PCR products were digested with specific restriction enzymes (Appendix 6.1). An example of the reaction is shown in Table 2.7.

Table 2.7 - Digestion of *uroD* and pPr-IBA2 with KpnI and BamHI.

Compound	Final concentration	Brand
DNA (gene/plasmid)	≥20ng/µL	-
10x Cut Smart Buffer	1x	*New England Biolabs*®
KpnI – High Fidelity*	10-20 units per µg DNA	*New England Biolabs*®

BamHI – High Fidelity*	10-20 units per µg DNA	*New England Biolabs*®
MilliQ H_2O	Excipient qs.	-

*The enzymes used depended on gene/plasmid restriction site (Appendix 6.1).

The mixture was incubated at 37ºC for 1 hour and the digested fragments were purified using the QIAquick® PCR Purification Kit. The digested products were observed again in a 1% agarose gel.

Ligation

The digested PCR product and plasmid were ligated, using a T4 ligase, overnight at 16ºC. In Table 2.8 is described the mixture for the ligation.

Table 2.8 – Ligation of insert *uroD* into pPr-IBA2 plasmid.

Compound	Final concentration	Brand
Buffer T4 ligase	1x	*New England Biolabs*®
Insert DNA	0.060 pmol	-
Plasmid DNA	0.020 pmol	-
T4 ligase	5U/ µL	*New England Biolabs*®
Nuclease-free H_2O	Excipient qs.	-

The mixture incubates overnight at 16ºC to connect the fragments. The resulting ligated plasmid was transformed in *E. coli* ultracompetent cells and the positive clones selected by resistance plates with ampicillin. The constructed plasmid was extracted using miniprep and sent to sequence with primers flanking the inserted sequence (*STAB VIDA, Lda*.).

2. III. Preparation of competent cells and transformation

To increase the transformation efficiency, ultracompetent cells XL-1 were used to transform plasmids and obtain a high copy number. Therefore, stocks of -80ºC chemically pre-treated *E. coli* XL-1 ultracompetent cells were used.

E. coli ultracompetent XL-1 chemical treatment

For this pre-treatment, an overnight culture was diluted 1% in 25 mL of fresh LB and incubate at 37 ^{O}C, and 150 rpm, from 6 to 8 hours. After incubation, the culture was diluted at 0.04%, 0.4%, 1.6% and 4% in 4 flasks with 250 mL of fresh LB. The cultures incubated at 20 ^{O}C, and 150 rpm, overnight. The OD_{600} of these overnight cultures was measured every 45 min until OD_{600} ~ 0.55.

After an incubation of 10 min on ice, the cells were harvested at 2 500 *x g*, for 10 min at 4 ^{O}C. The supernatant was decanted, and the tubes dried for 2 min. The pellets were resuspended in 80 mL of ice-cold, sterile Inoue transformation buffer, and centrifuged at 2 500 *x g*, for 10 min at 4 ^{O}C. The supernatant was decanted again, and the tubes dried for 2 min. The cells were resuspended in 20 mL of ice-cold, sterile Inoue transformation buffer and 1.5 mL of DMSO was added and mixed. After an incubation on ice for 10 min, the cells were divided into 200 μL aliquots, flash frozen in liquid nitrogen and stored at -80 ^{O}C (Inoue, Nojima, & Okayama, 1990).

E. coli ultracompetent XL-1 transformation

Briefly, a pre-incubation with these cells and the plasmid in a ratio of 5:2 was done at 4ºC for ~30 min. The cells and the foreign DNA were placed at 42ºC for 45 seconds and again on 4ºC (ice) for 2 minutes for an "heat-shock", to permeate the cells membrane. Finally, incubation at 37ºC with agitation at 150 rpm for 1 hour took place in LB medium. The cells were harvested at 1677 *x g* for 5 minutes, and cellular sediment resuspended in the supernatant.

Plates with LB-agar containing the specific antibiotic for plasmid selection were used to plate the resuspended sediment. The plates incubate overnight at 37ºC.

To obtain pure cultures, a few colonies from the transformation plate were reisolated and streaked in a new LB-agar plate. Incubation was overnight at 37ºC.

The colonies were screened to select positive clones. Therefore, for each transformation, at least 4 good colonies were selected from the reisolation plate. The cells were lysed with boiling water (100ºC) and a colony PCR was performed using a similar protocol as in Table 2.5, except for the Taq DNA Polimerase enzyme *New England Biolabs*®, and its specific Thermopol buffer *New England Biolabs*®.

The size verification was possible through 1% electrophoresis agarose gels:

The pPr-IBA2(*uroD*) PCR product was acquired using primers 1 and 2 (Appendix 6.1).

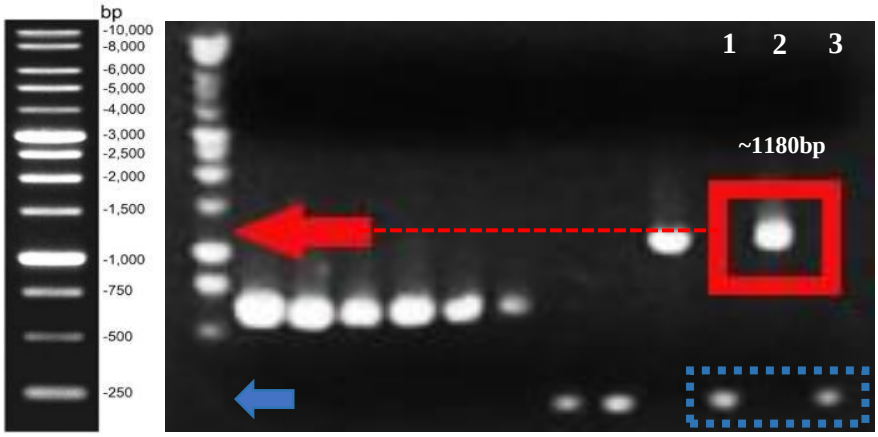

Figure 2.2 - Eletrophoresis for screening of pPr-IBA2_*uroD* positive clones. The *uroD* gene has 1023bp and the plasmid fraction is around 157 bp. The numbers 1, 2 and 3 represents pPrIBA2_*uroD* transformants. The red square (2) represents a positive plasmid (~1180bp), and the blue squares (1 and 3) are empty plasmids (~ 250bp).

The clone from the red square in Figure 2.2 had the correct size (~1180bp) and was selected to transform into the *E. coli uroD* mutant.

The pPr-IBA2(*ppfC*) PCR product was obtained using primers 10 and 11 (Appendix 6.1).

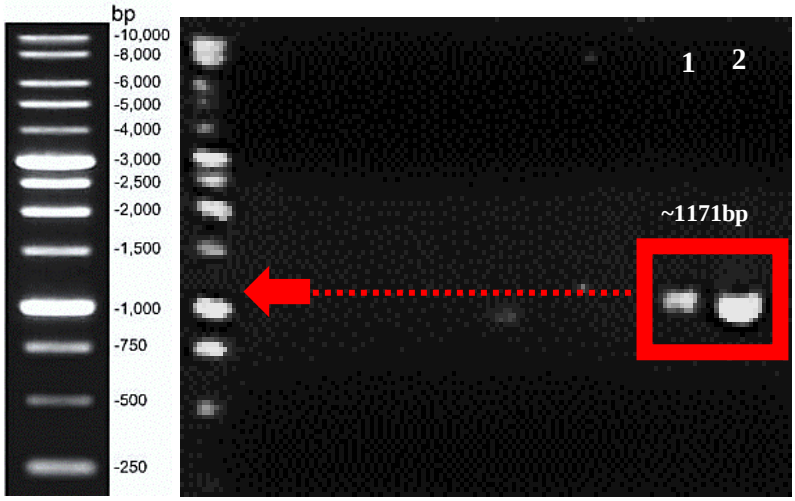

Figure 2.3 - Eletrophoresis for screening of pPr-IBA2_*ppfC* positive clone. The *ppfC* gene has 963bp and the plasmid is around 208 bp. The red squares (1 and 2) represent transformants with a positive plasmid of pPrIBA2_*ppfC* transformants.

In Figure 2.3, the clones from the red squares were used to transform Δ*ppfC* due to size expectation (~1171bp).

The pPr-IBA2(*cgdH*) PCR product was cloned using primers 4 and 5 (Appendix 6.1).

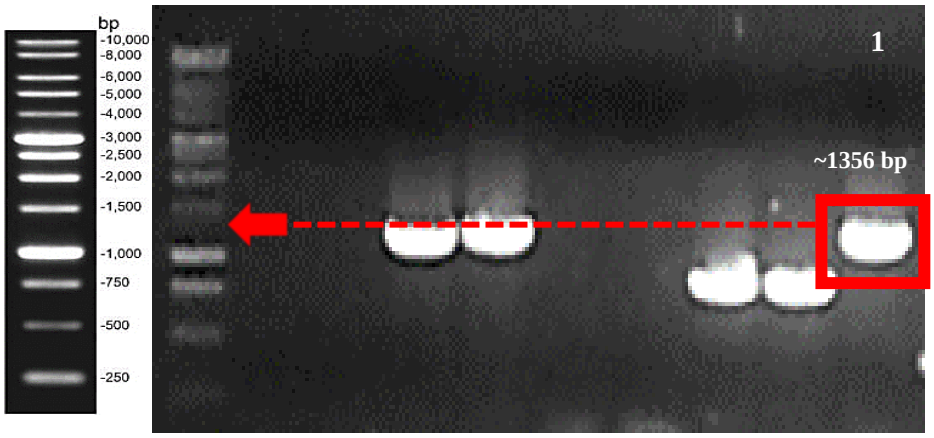

Figure 2.4 - Eletrophoresis for screening of pPr-IBA2_*cgdH* positive clone. The *cgdH* gene is about 1356bp. The red square (1) represents a positive plasmid of pPrIBA2_*cgdH*

The clone from the red square in Figure 2.4 is a positive plasmid of pPr-IBA2(*cgdH*) that was used to transform Δ*cgdH* due to similar size expectation (close to 1356bp).

The positive plasmids were purified with QIAprep® Spin Miniprep kit, using 4mL of a prepared overnight culture for each were centrifuged at 6800 *x g* for 3 min at room temperature. The pelleted bacteria were resuspended, lysed, and neutralized to obtain a concentrated plasmid DNA with an elution of 50µl of MQ H_2O.

E. coli hem$^-$ mutants chemical competence and heat shock transformation

Overnight cultures of *E. coli* Δ*uroD*, Δ*ppfC* and Δ*cgdH* mutant strains were inoculated at 1:100 in 10mL fresh LB medium with (21mM) $MgCl_2$ and (20mM) $MgSO_4$ treatment. Cells were incubated at 37ºC at 150rpm until OD_{600} ~ 0.6. The culture was placed on ice for at least 10 minutes. All further steps were performed at 4ºC.

For each transformation, the cells of 2mL of inoculum were harvested at 4293 *x g* for 10 minutes. The pellet was resuspended in ice-cold, sterile TB buffer (10mM HEPES, 15mM $CaCl_2$, 250mM KCl and 55Mm $MnCl_2.4H_2O$ pH 6.7, adjusted with KOH) in a ratio of a third of the volume of inoculum used. The suspension was further incubated on ice for 10 minutes and centrifuged at 4293 *x g* for 10 minutes. The pellet was resuspended again in ice-cold, sterile TB buffer (the same volume of overnight culture added initially).

The subsequent transformation protocol of the plasmids into *E. coli* hem$^-$ mutants was the same described above in the section 2. III.

To obtain isolated colonies, 6-10 transformants were reisolated into a new LB-agar plate. Stocks were prepared with culture in LB liquid medium (75%) and glycerol (25%) and stored at -80ºC.

2. IV. Complementation assays

Complementation with solid media

In solid media, colonies from the strains were streaked, side-by-side, using a tip. Ampicillin was added and increasing concentrations of haemin (at least two for each strain, 0 µM and 10 µM). The plates were incubated overnight at 37ºC on a dark place.

To serial dilutions in solid media, *E. coli* strains cell cultures were grown overnight as already described in the presence of haemin. Before serial dilutions, the overnight cultures were previously washed with PBS buffer, by pelleting 1 mL of culture and resuspending in PBS buffer 3-5 times.

Using the previous suspension, further stepwise dilutions were done in 1:10 to obtain dilutions from 10^0 to 10-8. A 5 µL drop of each dilution was dropped on LB plates with ampicillin and different concentrations of haemin. All strains were spotted on the same plate. The plates were incubated overnight at 37ºC on the dark, to avoid degradation of haemin and the Δ*ppfC* mutant sensitivity to light.

Complementation in liquid media

The complementations were done in the liquid media using 1/10 of the volume of pre-inoculums of each strain. After centrifugation, the cells from 1 mL bacterial pellet were washed by resuspension 2-3 times in the same volume of PBS buffer. The cells were diluted in fresh LB-media with ampicillin to start with OD_{600} = 0.05. Two different flasks were prepared for each strain, and 10µM of haemin was added to one of them. The inoculum was incubated at 37ºC and 180rpm, and the OD_{600} was measured every hour to trace a growth curve.

Haem staining assay

Pre-inocule of the strains used in these assays were grown in M9 minimal medium supplemented with glycerol 0.4% (v/v), fumarate 40 mM, thiamin 1µg/mL, casaminoacids 0.2% (v/v), TMAO 20mM and NO_2^- 2.5mM (as mentioned in Table 2.4). Cell were grown under anaerobic conditions at 37ºC, without agitation, for ~ at least 20 hours.

These cells were used to fresh medium and grown anaerobically at 37ºC for more ~20 hours. The cells were harvested at 10 000 *x g* for 10 minutes, the dry weight was measured, and the pellets were washed with PBS buffer to a final concentration of 200mg of cells/mL. Then, cells were disrupted in a French Press at 900 psi. An alternative way to disrupt and analyse the cell extracts was used, by boiling 100 µL of PBS-resuspended cell pellet in water for 10 minutes. A sample of the cell extracts was taken

and resuspended in loading dye without ß-mercaptanol. Then 20 µL of each sample was loaded into a 15% SDS-PAGE gel. The electrophoresis was set to run for 1 hour at 150 mV.

To determine the protein content, gels were stained using coomassie blue R-250 staining – coomassie brilliant blue R-250 powder 3g/L, methanol 45% (v/v), glacial acetic acid 10% (v/v) and destilated water 45%. To reveal haem-binding proteins SDS-Page gels were stained using tetramethylbenzidine (TMBZ) staining. The gel was immersed in TMBZ staining solution (3 parts of TMBZ 6.3mM in methanol and 7 parts of sodium acetate 0.25M pH 5) and covered with aluminum foil at room temperature for 1 hour with occasional agitation. Hydrogen Peroxide (H_2O_2) was added to the final concentration of 30mM and left by 30 minutes to increase stain intensity. The gel was destained using an acetate-buffered 30% isopropanol solution (3 parts of isopropanol and 7 parts of sodium acetate 0.25M pH 5). The solution was replaced twice to remove the TMBZ precipitate, clear the background and enhance the staining intensity.

Nitrite consumption assay

For the NO_2^- consumption assay the strains grew overnight in M9 minimal medium supplemented with glycerol 0.4% (v/v), fumarate 40 mM, thiamin 1µg/mL, casaminoacids 0.2% (v/v) (Table 2.4). The cultures were inoculated at 1% in the same media conditions and were grown anaerobically, at 37ºC, for 3 hours. Duplicates were done for each strain and NO_2^- was added in one of them.

To the determination NO_2^- concentration, the Griess method was used (Giustarini, Rossi, Milzani, & Dalle-Donne, 2008). First, a calibration curve was traced using a NO_2^- solution that ranged from 0 to 25 µM in a 10 points scale. Then the culture samples and the calibration curve were loaded in a 96-well plate and were mixed with the Griess reagent (1% Sulfanilamide and 0.1% Naphthylene diamine dihydrochloride resuspended in 30mL of MQ H_2O and add 2% H_3PO_4) in a proportion of 1:2. Absorbance at 540 nm was measured in a plate reader.

Coproporphyrin III quantification

To quantify coproporphyrin III in cells, 1% of overnight cultures were inoculated in LB medium with kanamycin and incubate anaerobically at 37ºC for 48 hours. The cells were harvested at 54234 *x g* for 15 minutes, at 4ºC. The cells received two different treatments to extract compounds for the High-Performance Liquid Chromatography (HPLC) experiments: ethyl acetate/glacial acetic acid and HCl extracting methods.

For the ethyl acetate/glacial acetic acid method, the pellet of 2L culture was resuspended in 30 ml of ethyl acetate/glacial acetic acid/H_2O (2:1:1, v/v) and protected from the light. The cells were lysed

by French Press at 900psi and centrifuged at 48298 *x g* for 30 minutes (4ºC). The supernatant was collected, and the pellet washed with 4 ml of ethyl acetate/glacial acetic acid (3:1, v/v). The supernatant and the main ethyl acetate fraction were combined. This product was concentrated by SpeedVac until dryness. The samples were resuspended in 300µL of running solvent (20% Acetonitrile; 80% TFA (0.1%)) and injected in a Kromasil C18 column (dimensions 10 x 250 mm) into the Agilent 1100 HPLC with a flow rate of 0.2 mL/min.

For the HCl extraction method, cells were collected, as in the ethyl acetate/glacial acetic acid method. The pellet resuspended in phosphate K^+ buffer 20mM and lysed by French Press 900psi. The lysates were centrifuged 48298 *x g* for 30 minutes at 4ºC. The supernatant was concentrated in SpeedVac until 1mL. To precipitate the proteins, HCl was added to a final concentration of 0.6M. The samples were mixed by vortex for 10 minutes and centrifuged them at 6708 *x g* for more 10 minutes. More a less 300µL from the supernatants were injected in the column in the HPLC, that ran with a flow rate of 0.2mL/min.

To summarise this Materials and Methods section, Figure 2.5 shows a resume of the followed practices in materials and methods to obtain the results mentioned in the next section.

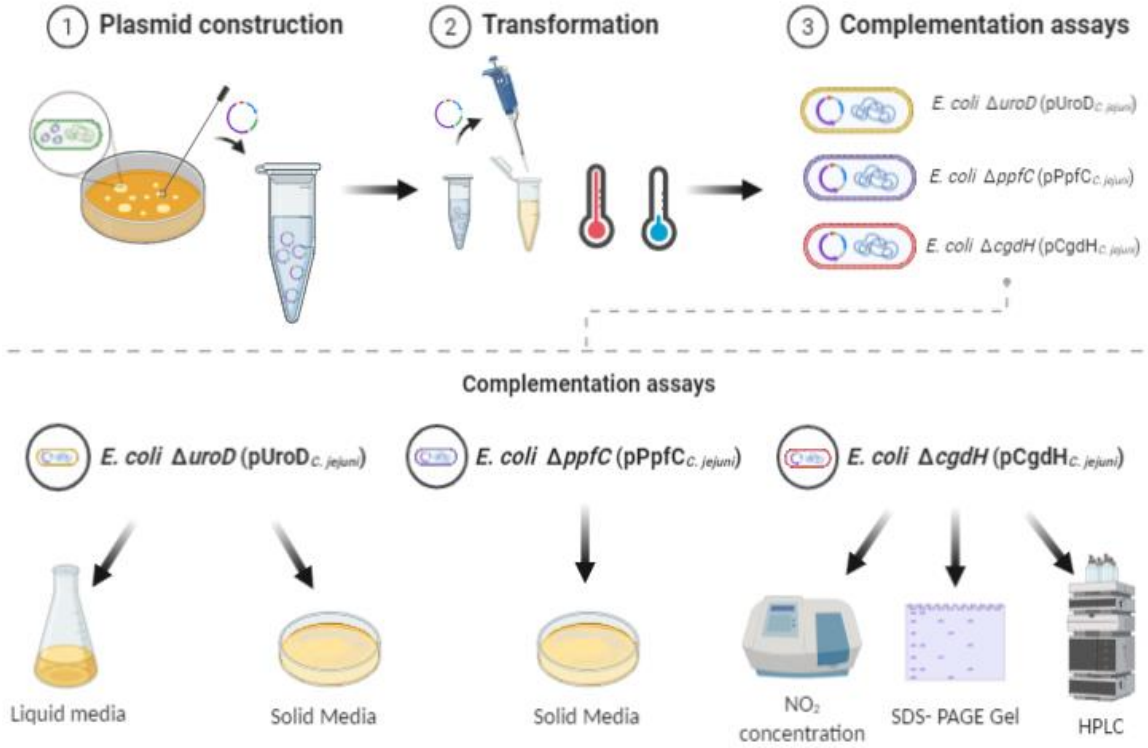

Figure 2.5 – Flowchart of the performed laboratory work. Plasmids constructions (1) were used to transform mutants (2) and perform complementation assays (3).

3

Results and discussion

This section shows the results and discuss to main outcomes and contributions of my work to this project.

The main goal of this study is to unravel the functional haem biosynthesis pathway of *C. jejuni*. The putative enzymes responsible for the haem biosynthesis pathway in *C. jejuni* were identified by using a bioinformatic analysis, prior to my arrival in the laboratory. The enzymes identified were UroD, PpfC, CgdH, PgdH2 and PpfC and they are associated to a putative PPD pathway (Table 3.1 and Figure 3.1). However, up to date there is no data available about the function of these enzymes. Thus, the aim of this work will contribute to answer the question "What is the role of these *C. jejuni* enzymes in haem biosynthesis?".

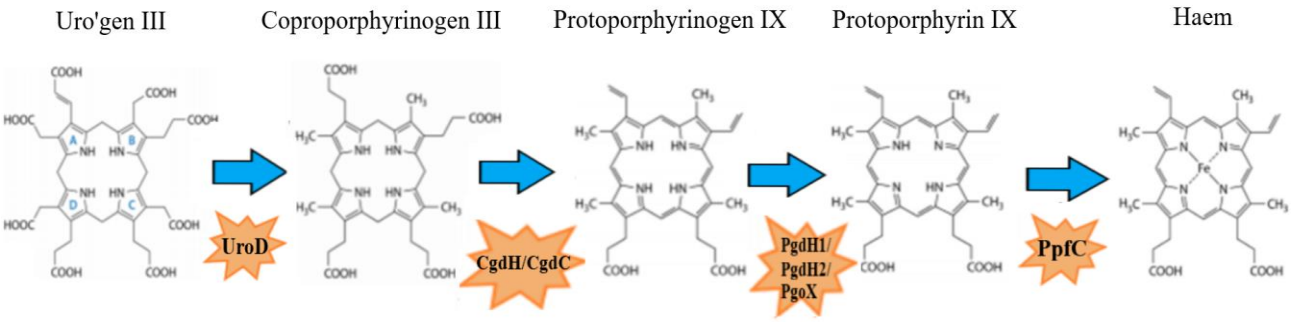

Figure 3.1 - The Protoporphyrin Dependent pathway (PPD). Schematic representation of the protoporphyrin pathway with the enzymes that catalyse each of the steps until the formation of haem.

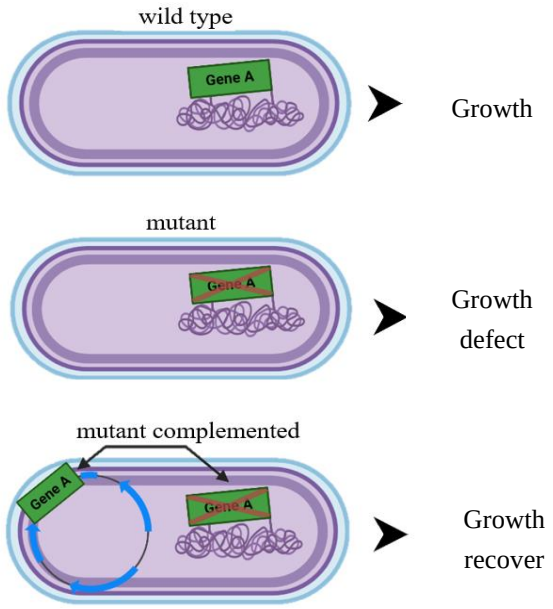

Figure 3.2 - Genetic complementation approach. Example of a genetic complementation. In this example, the wild type strain can grow normally under these conditions while possessing *gene A*. When *gene A* was deleted, a phenotype of growth defect appeared. This effect was reversed by complementing in trans with a plasmid carrying the *gene A*. These results show us that *gene A* is the gene responsible of the growth defect observed in the mutant strain.

E. coli, a Gram-negative bacterium commonly used as bacterial model for decades, also possesses this pathway. Therefore, to answer the question, a stepwise genetic complementation approach was used in *E. coli*.

Indeed, in *E. coli* the function of most of the PPD pathway enzymes have been elucidated, the mutant strains of each enzyme are available, and both genetic manipulation and growth is much easier than in *Campylobacter jejuni*. Therefore, for the mentioned reasons, doing the complementation assays in *E. coli* will be the most affordable way to better understand the role of each enzyme of the *C. jejuni*'s haem biosynthetic pathway. The role of UroD, CgdH and PpfC enzymes in haem biosynthesis was analysed.

For the genetic complementation, an *E. coli* wt strain with no haem deficiency and a mutant strain with a deletion of an essential gene to haem biosynthesis were used. Later, this mutant was complemented with a plasmid containing the essential gene and the growth is restored (Figure 3.2). In this case, *E. coli*'s mutant strains of the PPD pathway were used and complemented with an expression vector containing the putative equivalent *C. jejuni*'s enzymes, expecting to revert the phenotype.

Table 3.1 - Putative genes of *C. jejuni* haem biosynthesis pathway.

Gene name	Old name	KEGG code
uroD	*hemE*	*cj1243*
cgdH	*hemN*	*cj0992c*
pgdH2	*hemJ*	*cj0362*
ppfC	*hemH*	*cj0503c*

3. I. UroD from *C. jejuni* is a functional uroporphyrinogen III decarboxylase

Plasmid constructions

To perform the complementation assays, plasmids harbouring each of the genes belonging to the haem biosynthetic pathway of *C. jejuni* were constructed. These individual plasmids expressing *C. jejuni* genes (*uroD, cgdH, pgdH2*, and *ppfC*)(Table 3.1) were constructed using the pPr-IBA2 plasmid.

Complementation assays

In this chapter, the $UroD_{C.jejuni}$ uroporphyrinogen III decarboxylase activity was analysed. To do so, *E. coli* Δ*uroD* strain was complemented with a pPr-IBA2 plasmid containing $UroD_{C.jejuni}$. An *E. coli* Δ*uroD* strain is not able to grow in LB under aerobic conditions without an external source of haem. The hypothesis is that if $UroD_{C.jejuni}$ possesses uroporphyrinogen III decarboxylase activity, then the overproduction of UroD *C.jejuni* in a Δ*uroD E. coli* strain would restore this growth defect.

First, the complementation assays were performed in liquid media. For that purpose, the *E. coli* Δ*uroD* mutant strain harboring *uroD C.jejuni* (p$uroD_{C.jejuni}$) or the empty plasmid (pØ) were grown in LB medium in the presence or absence of haemin and measured the OD_{600} value overtime to monitor the growth of the strains for 7 hours. As a control, an *E. coli* wt strain with the empty plasmid have grown in parallel. Figure 3.3 shows that the wt strain reached the log phase after 1h of growth and the stationary phase after 3h of growth, during this lapse of time the OD_{600} values increased by 1-2 log in both conditions with and without haemin. On the other hand, the Δ*uroD* pØ and Δ*uroD* p$UroD_{C.jejuni}$ mutant strains log phase ranged from 1h to 6 h and the OD_{600} values increased by only 1 log. these results showed that the *E. coli* Δ*uroD* pØ strain possess a growth defect when grown in LB medium. However, the addition of haemin in the medium did not suppress such phenotype. Strikingly, complementation with the p$UroD_{C.jejuni}$ plasmid did not suppress this grow defect neither.

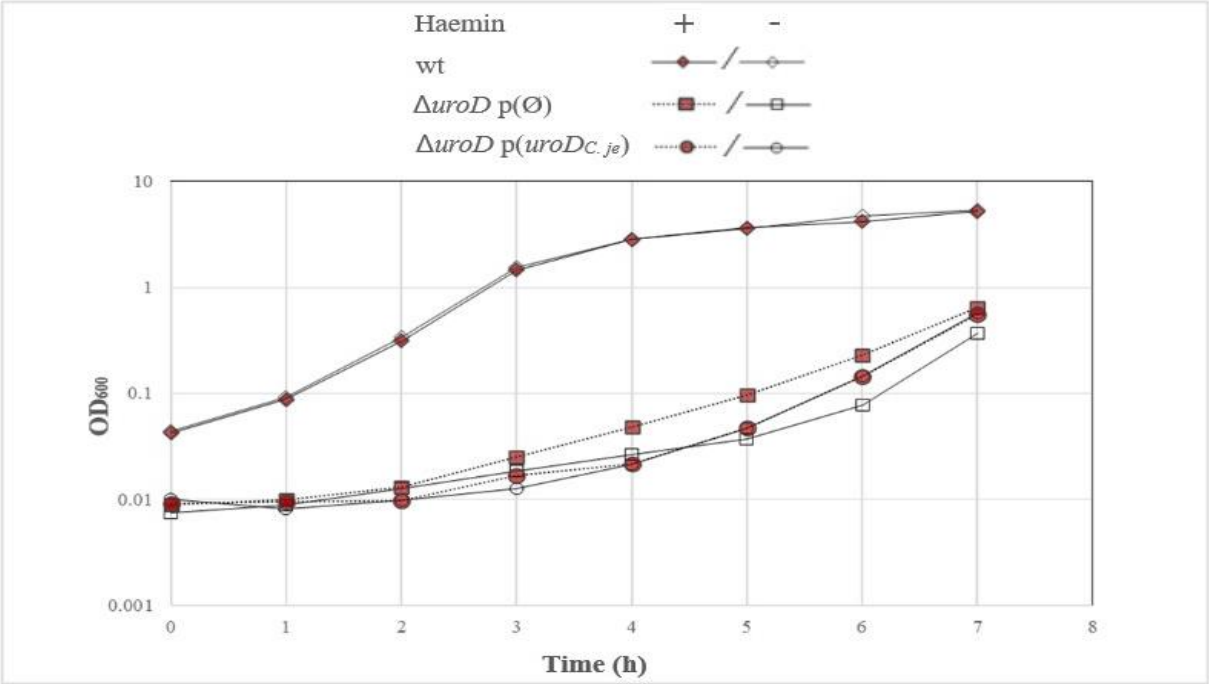

Figure 3.3 - Δ*uroD* complementation. The wt (diamonds shape), Δ*uroD* pØ (squares), Δ*uroD* pUroD$_{C.je}$ (circles) were grown with (red filled) or without (white filled) haemin (10µM). OD_{600} values were analysed every hour for seven hours.

Therefore, even though the plasmid overexpressing UroD$_{C.jejuni}$ did not complement the growth defect of a Δ*uroD* strain, this growth defect was not suppressed by the addition of hemin. Thus, it is not possible to conclude on the results observed for this liquid media complementation assay.

Complementation in viability assays

The complementation assays in solid media were then performed. In this case, the cells were grown overnight, aerobically in 1:10 LB-media, with antibiotic and haemin. Then, the strains were streaked or used to perform serial dilutions and spotted in LB-agar plates supplemented or not with hemin.

It is noteworthy to say that before starting the experiments it was necessary to adjust the haemin concentration to perform the tests because bacterial strains are sensitive to the relative haemin concentrations and an excessive amount can be ineffective or toxic for the cell.

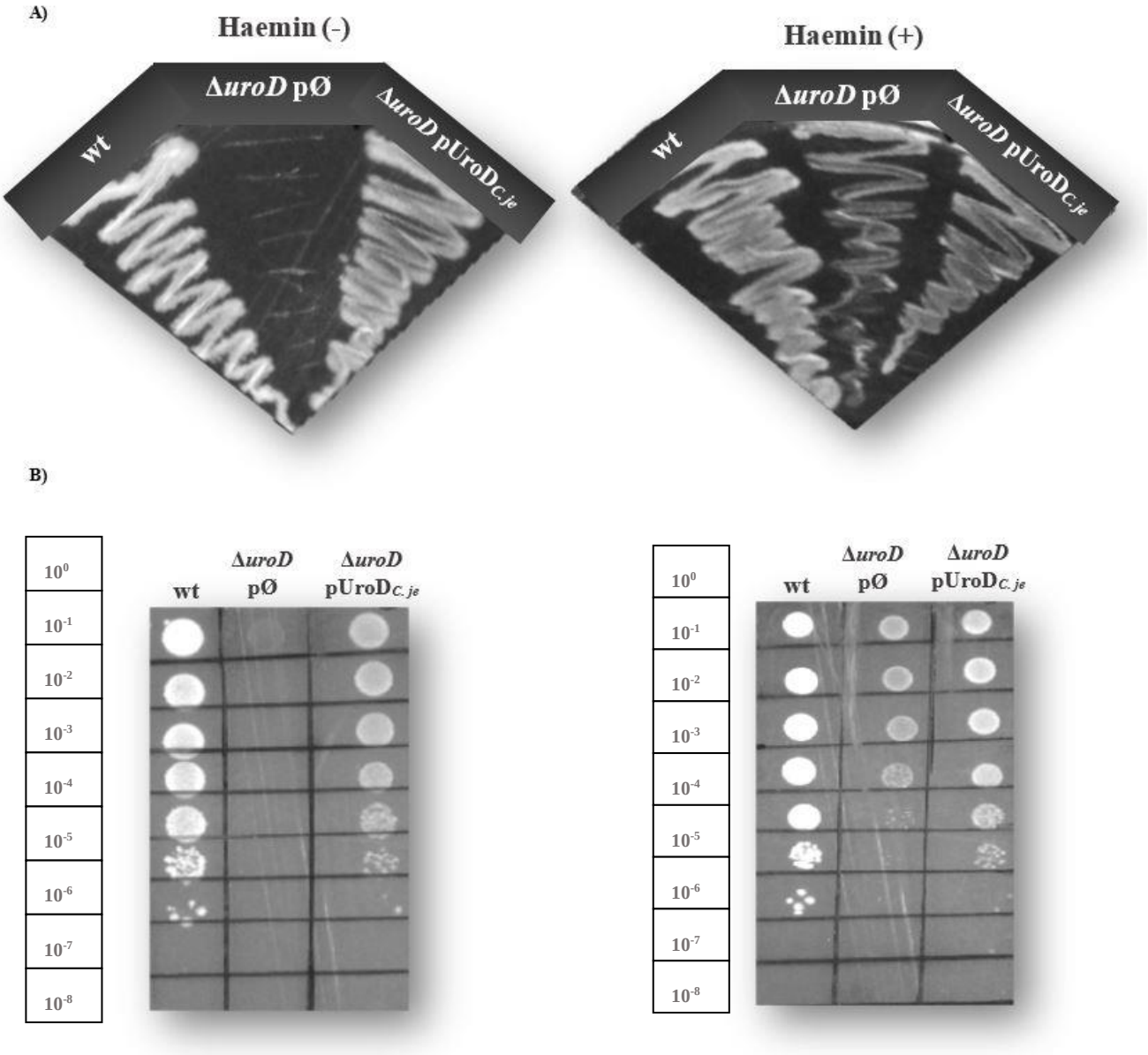

Figure 3.4 - Δ*uroD* complementation in solid media. The wt, Δ*uroD* pØ and Δ*uroD* pUroD$_{C.je}$ strains from *E. coli* were grown in LB plates in the presence or absence of haem. Growth was analysed by streaks (A) or serial dilutions (B).

In Figure 3.4 it is possible to observe that overproduction of UroD$_{C.jejuni}$ rescues the growth defect of an *E. coli* Δ*uroD* strain. In panel A only the wt and the Δ*uroD* pUroD$_{C.jejuni}$ strains can grow in the absence of haemin, whereas when hemin was supplemented into the medium the Δ*uroD* strain was also able to grow. A similar result was observed with serial dilutions shown in panel B. Thus, showing that the pUroD$_{C.jejuni}$, can complement the *E. coli* Δ*uroD* strain.

In this section, the growth rates of an *E. coli* Δ*uroD* strain in liquid medium were first analysed. In this case, the p*uroD*$_{C.jejuni}$ plasmid did not have a positive effect in the *E. coli* Δ*uroD* strain growth

rate, thus suggesting that UroD$_{C.jejuni}$ would not be able to complement such strain. However, the fact that the addition of haemin did not have any positive effect on the growth rate of the *E. coli* Δ*uroD* strain, did not allow to extract any conclusions from the results observed. Later, the same strategy was used but this time by plating in solid medium containing or not haemin. Interestingly, this time it was not possible to observe that a strain defective in uroporphyrinogen decarboxylase activity could not grow in the absence of an external source of haem but when complemented with UroD from *C. jejuni,* this fully restored bacterial growth, and in this case the addition of haemin also restored growth in the *E.coli* Δ*uroD* strain.

Overall, the results indicate that the UroD enzyme from *C. jejuni* possess uroporphyrinogen decarboxylase activity.

3. II. PpfC from *C. jejuni* is a functional protoporphyrin ferrochelatase

In this second chapter, the protoporphyrin ferrochelatase activity of the putative PpfC enzyme was analysed. To do that, a Δ*ppfC E. coli* strain was complemented with the pPr-IBA2 plasmid containing PpfC$_{C.jejuni}$ (pPpfC$_{C.jejuni}$). As stated before, this *E. coli* mutant lacks the *ppfC* essential gene to produce haem and is not able to grow aerobically, in LB without addition of haem source. Hence, it was presumed that if the PpfC enzyme from *C. jejuni* possesses ferrochelatase activity, its overproduction will restore the growth defect of the Δ*ppfC E. coli* strain.

Complementation in viability assays

Solid media was used to analyse the complementation of Δ*ppfC* strain. The activity of the putative protoporphyrin ferrochelatase from *C. jejuni* in an *E. coli ppfC* defective strain was tested. As mentioned before, the growth was analysed by performing streaks and serial dilutions in plates supplemented or not with haemin (10μM). The Δ*ppfC* strain is also light-sensitive, which made manipulation of the strain more intricated.

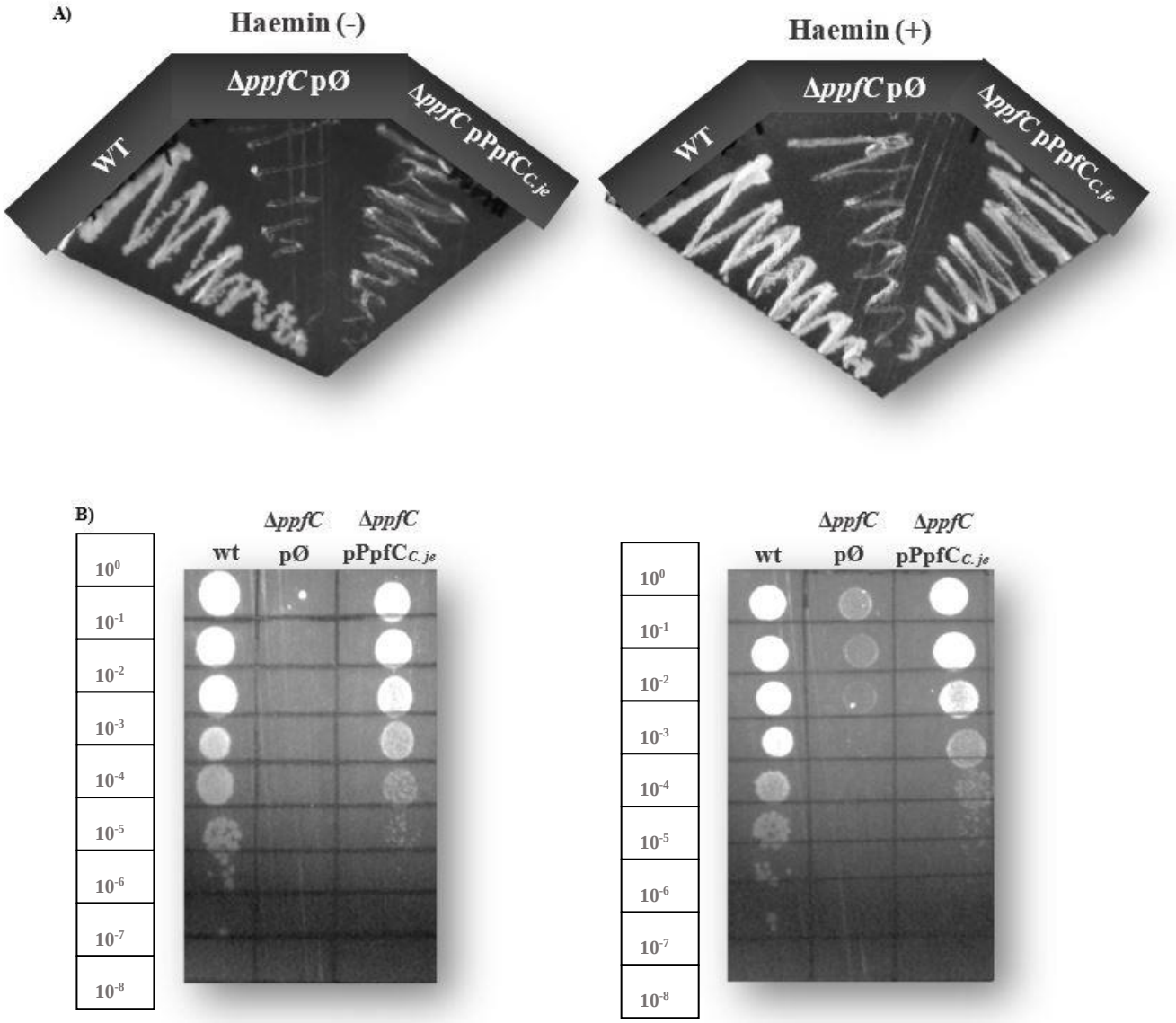

Figure 3.5 - Δ*ppfC* complementation in solid media. The wt , Δ*ppfC* pØ and Δ*ppfC* pPpfC$_{C.jejuni}$ strains from *E. coli* were grown in LB plates with or without haem source. Growth was observed by streaks (A) or serial dilutions (B).

Figure 3.5 shows that overproduction of PpfC$_{C. jejuni}$ restored the growth deficiency of the *E. coli* Δ*ppfC* strain in the absence of haemin.

Thus, these results show that PpfC$_{C. jejuni}$ is a functional protoporphyrin ferrochelatase.

3. III. Testing coproporphyrinogen dehydrogenase activity of CgdH from *C. jejuni*

So far, the activity of UroD that performs the first step of the PPD pathway was assessed, and of PpfC that is responsible for the last step. These enzymes in *E. coli* are essential to the biosynthesis of haem, being the reason to give a strong phenotype when these genes are deleted. This is not the case of CgdH, for example, which performs the second step of the PPD pathway, just after UroD (Figure 3.1). Indeed, deletion of *cgdH* in *E. coli* has no effect in growth. Nevertheless, previous work with this gene described that the lack of *cgdH* in *E. coli* resulted in a decrease of nitrate reductase activity and in the amount of type c-cytochrome (Tyson *et al*., 1997) and in an accumulation of coproporphyrinogen III (Ji *et al*., 2019).

In this case, these phenotypes will be complemented to test the $CgdH_{C.\ jejuni}$ coproporphyrinogen III dehydrogenase activity. Therefore, the nitrate consumption rate was analysed, the relative amount of haem-containing proteins and coproporphyrinogen III accumulation on the *E. coli* Δ*cgdH* mutant.

Nitrite consumption assay

Tyson *et al.* 1997 observed that an *E. coli* strain lacking *cgdH* has its nitrite reductase activity highly reduced.

The hypothesis is that, if the nitrite reductase activity is affected, the nitrite consumption rate of a Δ*cgdH* strain would be reduced compared to a wt strain. If *C. jejuni*'s CgdH enzyme possesses coproporphyrinogen dehydrogenase activity, complementation of the *E. coli cgdH* mutant strain will restore the nitrite consumption rate. To test this, the nitrite consumption was measured and the growth under anaerobic respiratory conditions followed.

To analyse the nitrite consumption rate, wt and Δ*cgdH* strains were grown under anaerobic conditions in minimal medium. As carbon source glycerol was used and fumarate was the final electron acceptor to ensure anaerobic respiration. In addition, the medium was supplied with NO_2 and the growth followed over time, along with the NO_2 consumption.

A)

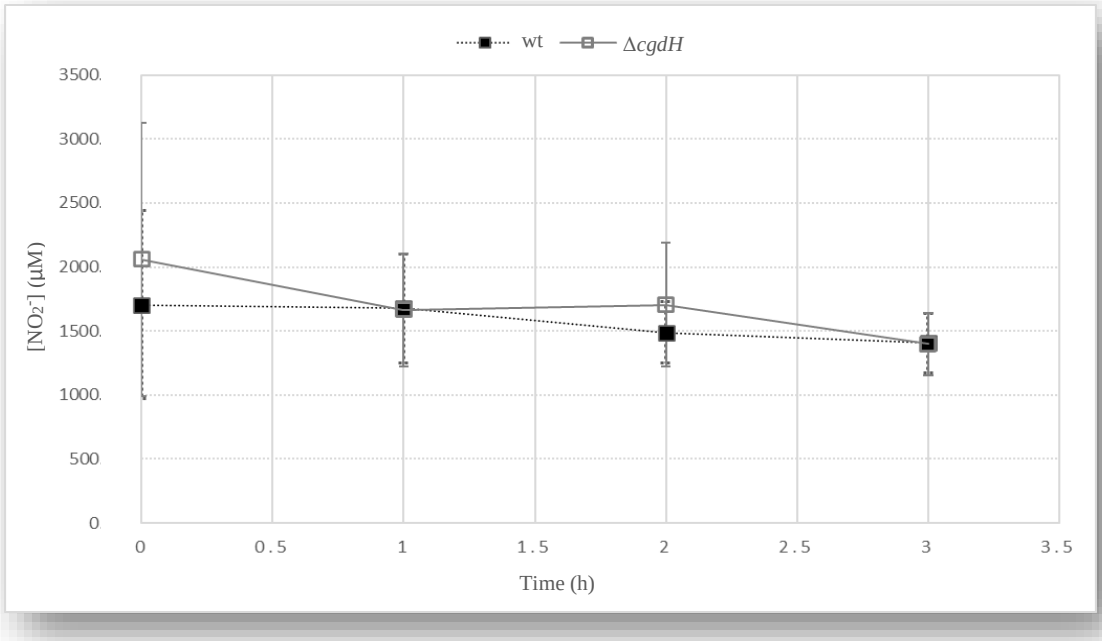

B)

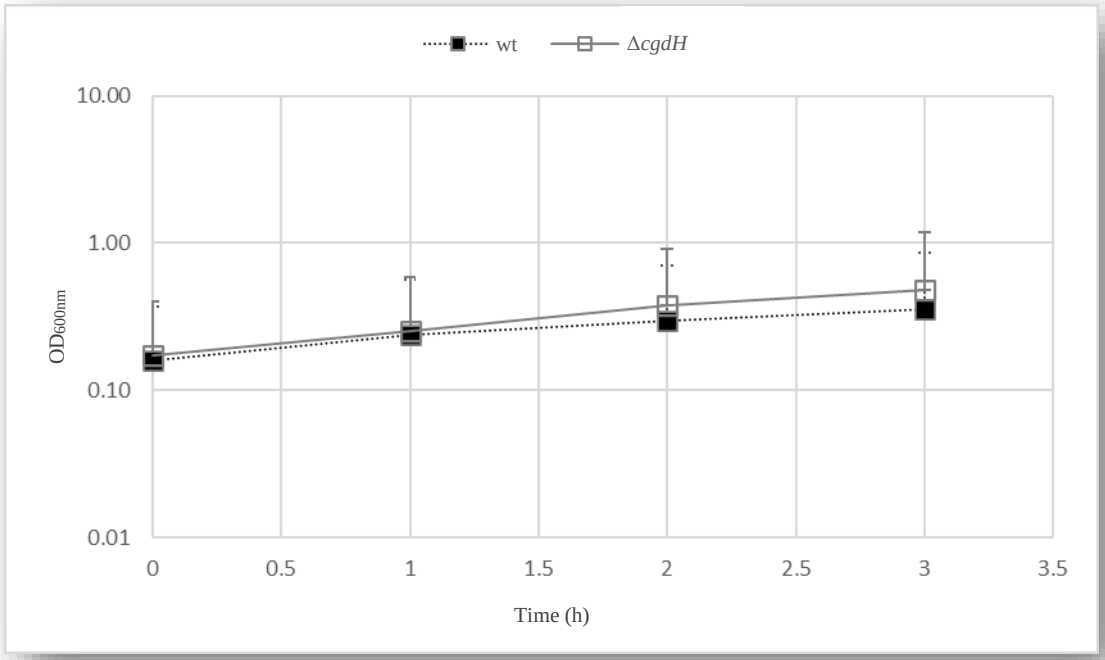

Figure 3.6 - NO_2 consumption assay. The wt and Δ*cgdH E. coli* strains were grown anaerobically in minimum media with glycerol, fumarate, and nitrite 2.5mM. Nitrite concentration in the media (A) and the OD_{600} (B) were measured every hour along 3 hours of growth at 37ºC.

Unexpectedly, and in contradiction to what is described in the literature, the results showed that the nitrite consumption rate of the Δ*cgdH* strain was similar to the wt strain. In Figure 3.6, after 3 hours of growth, the NO_2 concentration for the wt strain was ~1400µM and for the mutant strain 1400µM. Therefore, it was not observe any defect in nitrite consumption of the *E. coli* Δ*cgdH* strain.

The graphic in Figure 3.6 is a result of the average values of experiments of three different days. Therefore, the intact activity of *E. coli* Δ*cgdH* strain impaired testing the *C. jejuni* gene function.

Haem staining assay

In the same publication, Tyson and colleagues showed in 1997 that *E. coli* Δ*cgdH* strain is unable to synthesise any cytochromes during anaerobic growth (Tyson *et al*., 1997). A haem-staining protein gel revealed that under these growth conditions, the wt strain synthesis five-type c-cytochromes: NrfA, TorC, NapC, NrfB, and NapB. In contrast, the Δ*cgdH* strain is incapable of produce these proteins.

So, if the cytochromes synthesis is affected in the mutant, it is expected that the Δ*cgdH* strain did not reveal haem stained proteins when compared to a wt strain. If *C. jejuni*'s CgdH enzyme possesses coproporphyrinogen dehydrogenase activity, complementation of the *E. coli cgdH* mutant strain will restore the synthesis of these proteins.

Hence, the wt and Δ*cgdH* strains grew with fumarate and glycerol, under anaerobic conditions, and analysed the cytochrome content of the cell extracts. It is expected that using fumarate as a final electron acceptor and glycerol as a carbon source will stimulate metabolic pathways to obtain energy that requires enzymes that use haem as cofactor. In this way, haem-containing proteins will be produced in the respiratory chain of the wt strain, while the mutant will not be capable.

Two different approaches were followed to assess the NrfA, TorC, NapC, NrfB, and NapB proteins. The cells were disrupted by French Press or by boiling the samples in water. After running the samples in a sodium dodecyl sulfate-polyacrylamide gel electrophoresis (SDS-PAGE), the gel was stained with blue coomassie (to see the total protein content of the cell extract) and tetramethylbenzidine (TMBZ) staining, which will reveal the haem-containing proteins.

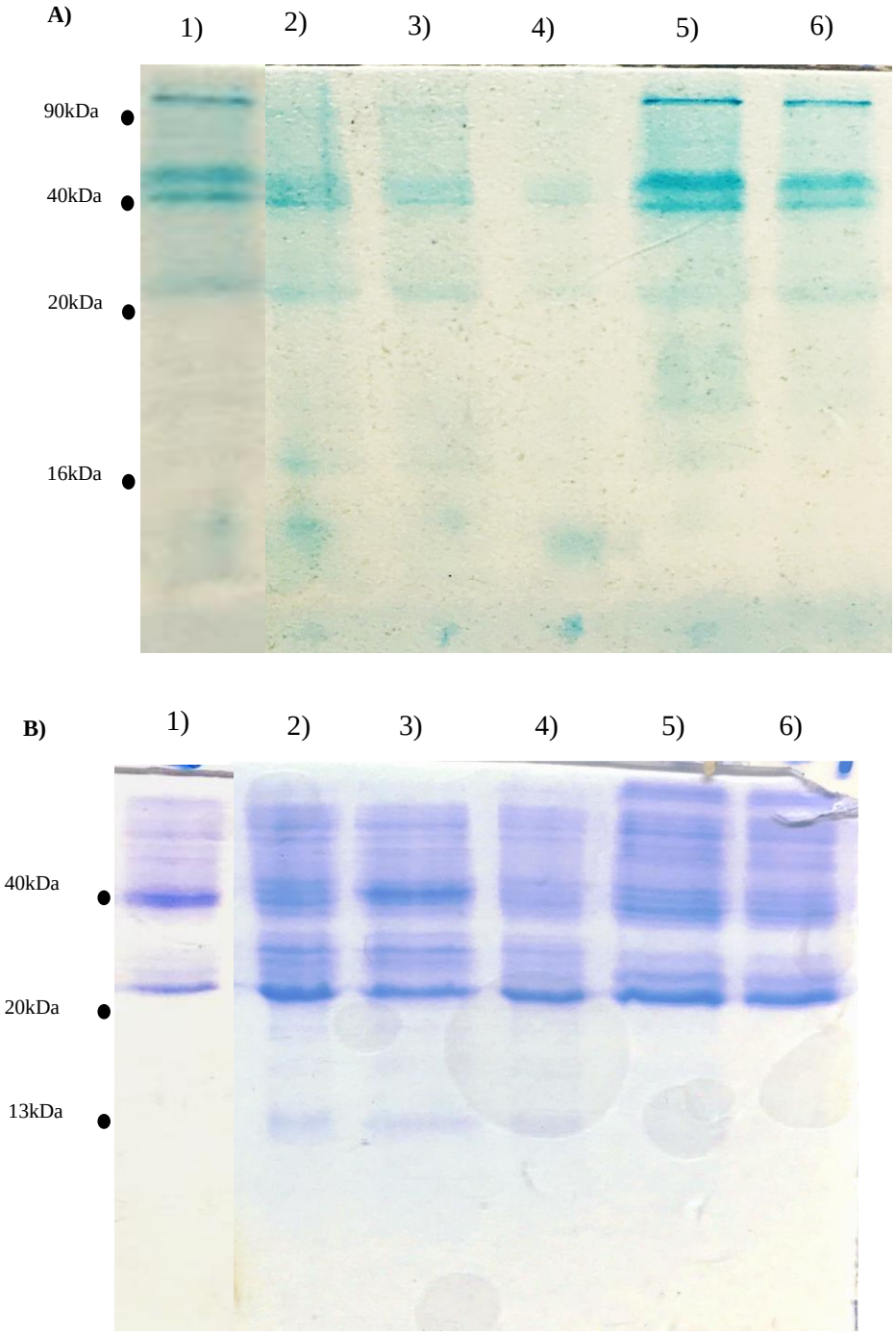

Figure 3.7- Haem staining purified proteins. The wt, Δ*cgdH* with the empty plasmid or with p*cgdH*$_{C.jejuni}$ were grown in minimal media under anaerobic fumarate respiration and in each lane was loaded 3mg of sample. The gels were stained TMBZ with (A) and coomassie blue staining (B). 1) Δ*cgdH*_p*cgdH*$_{C.jejuni}$ cells lysed with FP; 2) wt boiled cells; 3) Δ*cgdH*_pØ boiled cells; 4) Δ*cgdH*_p*cgdH*$_{C.jejuni}$ boiled cells; 5) wt cells lysed with FP; 6) Δ*cgdH*_pØ cells lysed with FP

In Figure 3.7A), it is shown that the TMBZ stained gel did not contain any haem-proteins below 40kDa for all the strains. The wt, the *cgdH* mutant and the complemented *cgdH* mutant have a similar haem stained protein profile. Furthermore, the blue coomassie gel presented only proteins above 20kDa, including the wt strain, which is not usually observed for *E. coli* (Figure 3.7B). So, it is not possible to trust these results to evaluate a potential $CgdH_{C.\ jejuni}$ activity.

Despite not seeing any differences between the strains, a better haem protein staining was obtained with the French press method in Figure 3.7.

After this first attempt, this experiment was replicated several times and ended up with a defined protocol. In this optimized protocol, the cells were broken through French Press to obtain the protein content.

In a last attempt, another experiment was designed in which the wt, the *cgdH* mutant and the *cgdC* mutant strains, were grown first aerobically, and then under anaerobic conditions, using fumarate respiration and glycerol as carbon source (Figure 3.8). A purified fumarate reductase flavoprotein (FccA) from *Shewanella putida* was loaded to have a positive haem-containing protein control.

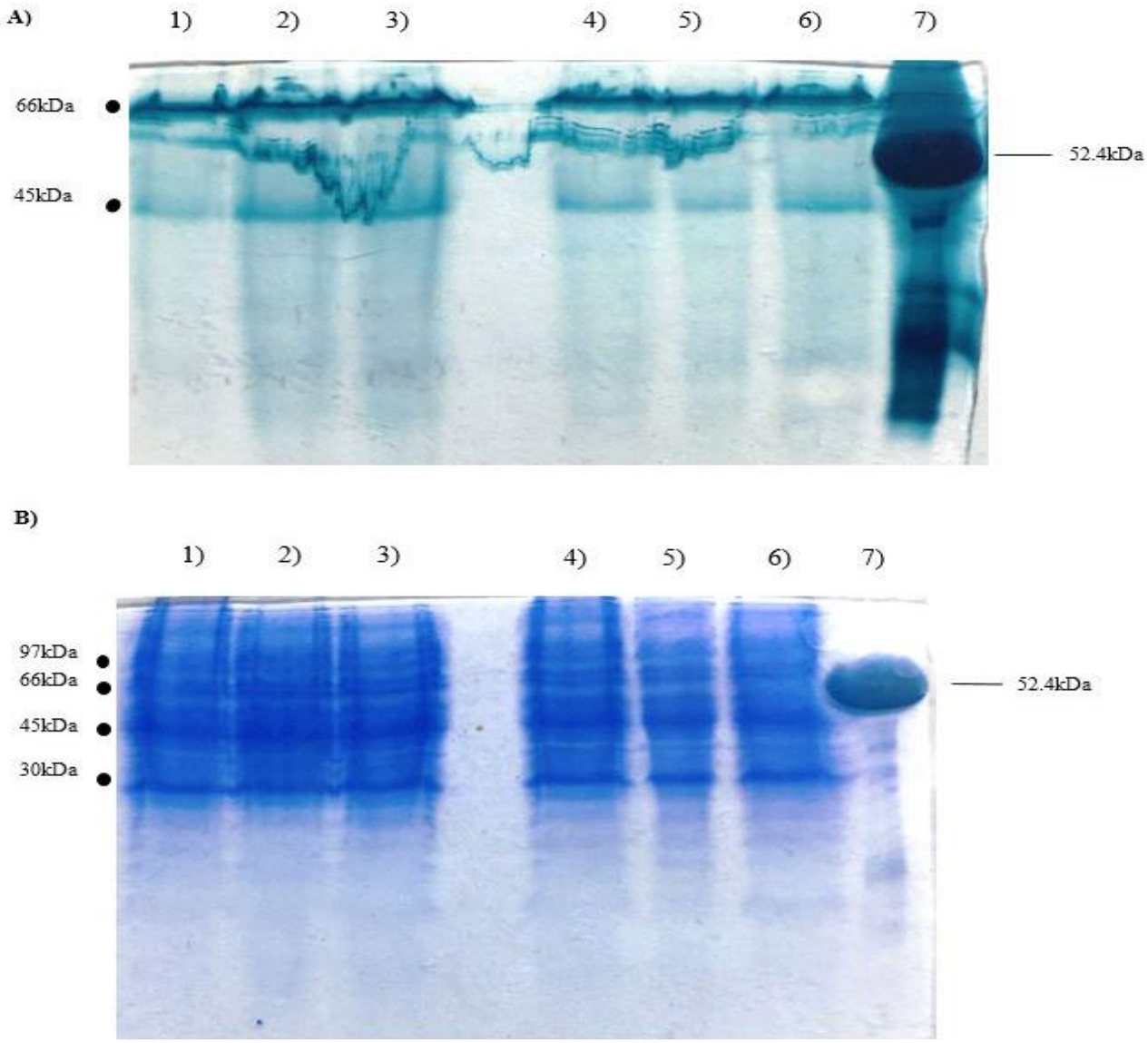

Figure 3.8 - Haem stained purified proteins. The wt, Δ*cgdH* and Δ*cgdC*, both with the empty plasmid, were grown under anaerobic fumarate respiration and in each lane was loaded 10 or 20µL of sample. The gels were stained with TMBZ staining (A) and coomassie blue (B). 1) wt strain (0.767mg/µL); 2) Δ*cgdC* pØ strain (2mg/µL); 3) Δ*cgdH* pØ strain (1.067mg/µL); 4) wt strain (0,767mg/µL); 5) Δ*cgdC* pØ (2mg/ µL); 6)) Δ*cgdH* pØ strain (1.067mg/µL); 7) Purified FccA*Shewanella putida* (haem protein control).

In the Figure 3.8, all samples were loaded with 20µl excepted for the lane 5 that was 10µL and the control in lane 7 that was 3µL. In A), some haem proteins lightly stained are detected in the wt, in the Δ*cgdH* and Δ*cgdC* strains between 66-45kDa. In B), the total content of proteins in the strains is shown and proteins only above 30kDa were observed. Consequently, the difference between in the *E. coli* Δ*cgdH* strain and the wt strain was not observed.

Again, the phenotype reported in literature could not be produced since the Δ*cgdH*_pØ mutant exhibited a similar haem-containing proteins profile than the wt strain.

In conclusion, the results do not show the reported phenotype of *E. coli* Δ*cgdH* mutant associated to cytochrome synthesis and it does not allow to evaluate the coproporphyrinogen dehydrogenase activity of the putative CgdH of *C.jejuni*.

Coproporphyrin III accumulation

According to Ji *et al.* 2019, an *E. coli cgdH* mutant accumulated coproporphyrin III. The same experiments were reproduced to analyse the porphyrin content of a Δ*cgdH* strain. To do so, two different methods to extract the coproporphyrin III from the cells were used. One that required the use of ethyl-acetate acetic acid treatment and another that requires the hydrochloride acid treatment (Ji *et al*., 2019; M. Videira *et al*., 2018).

To perform the experiment, the cells were grown anaerobically, and porphyrins were extracted from the wt strain and the *cgdH* mutant. The cell extracts that were injected in a HPLC column were analysed. The coproporphyrin III (5μM) was also injected in the column as control.

It is expected to observe peaks with a retention time similar to the one produced by the control sample. These peaks should be more pronounced in the *E. coli cgdH* mutant when compared to the parental strain to confirm this coproporphyrin III accumulation in the Δ*cgdH* strain.

First, the spectrum of coproporphyrin in the HPLC was analysed and showed a profile with a peak at 400nm with a retention time of 16.11 minutes (Figure 3.9). This compound profile worked as reference to compare with cell extracts from wt strain and the *cgdH* mutant.

A)

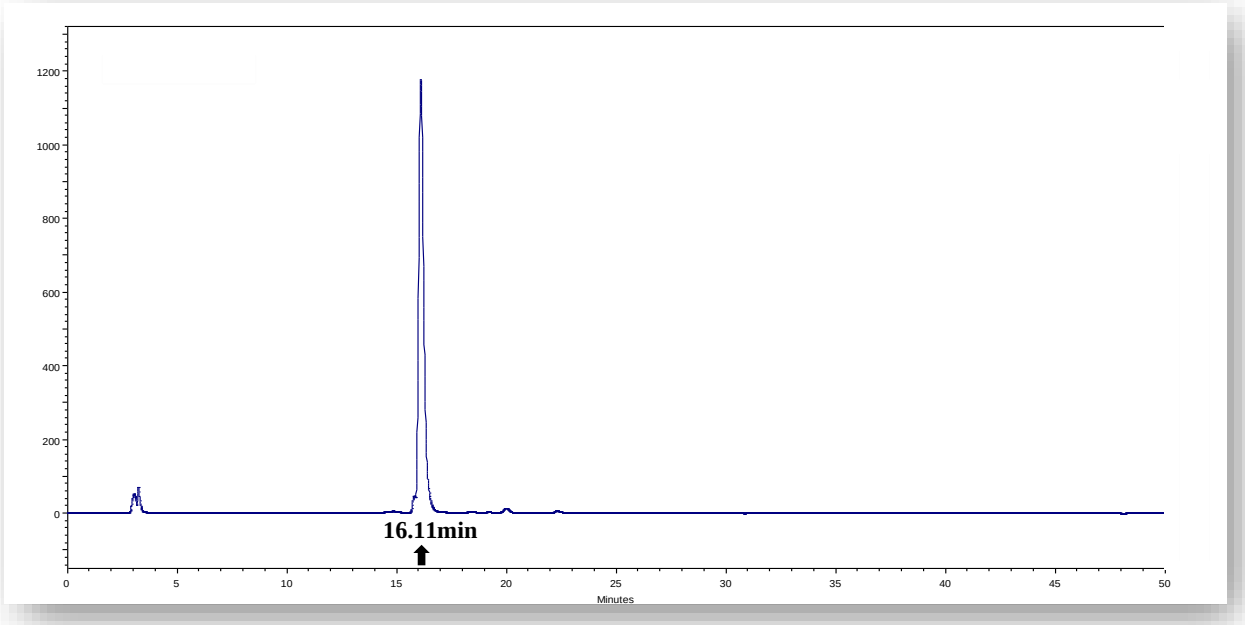

B)

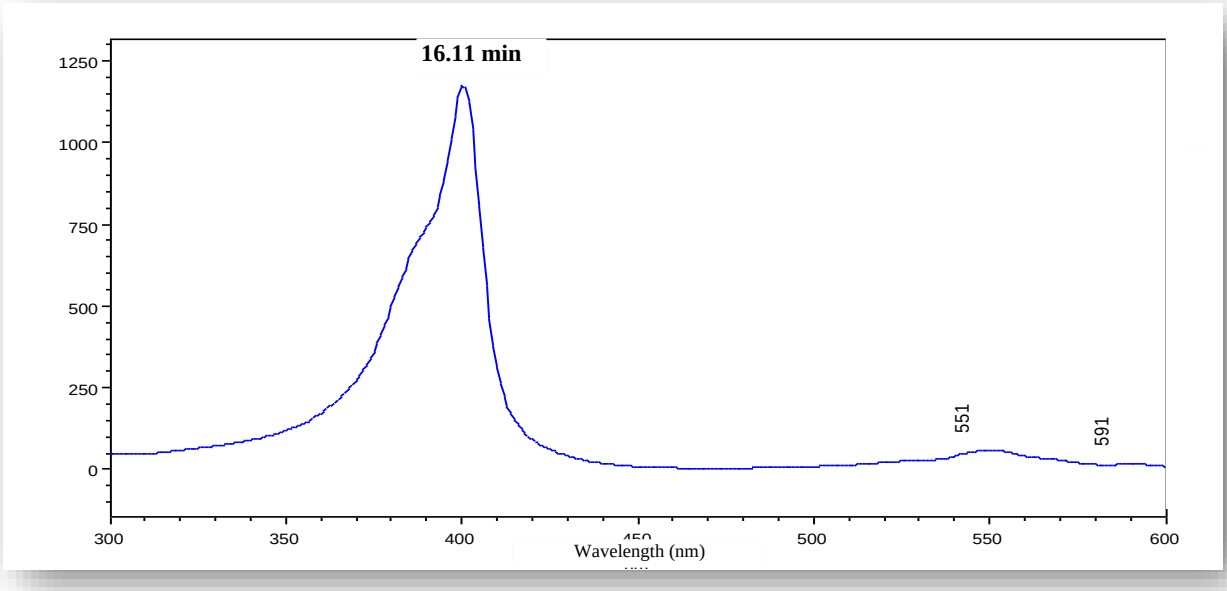

Figure 3.9 – HPLC-Coproporphyrin III elution's retention time of profile determination. Absorption spectra for coproporphyrin III eluted at 16.11 min (A) at 400nm (B).

The wt strain, obtained by the ethyl-acetate and acetic acid method (Figure 3.10) shows a simple broad peak at 15.46 min, at 400nm, that corresponds to coproporphyrin III.

The *E. coli* Δ*cgdH*_p*Ø* strain sample, processed by the ethyl-acetate and acetic acid treatment (Figure 3.11) show a wide speak at 15.51 min, with an absorption spectrum of 400nm, that resembles coproporphyrin III profile. Although several peaks were observed, the largest one is detected at 15.51 minutes.

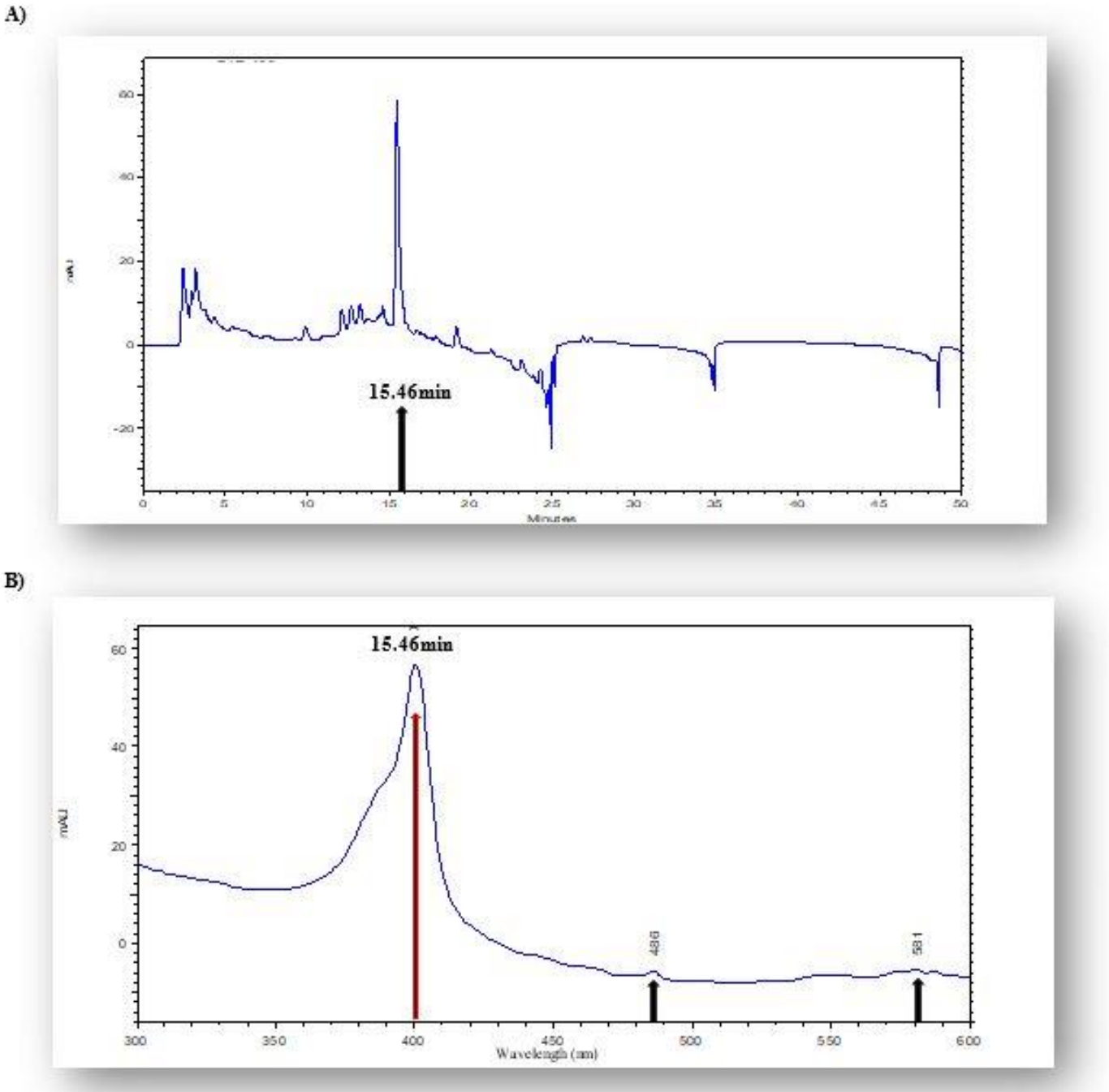

Figure 3.10- Analysis of the wt strain elution with the ethyl-acetate and acetic acid treatment. Absorption spectra for wt strain of the eluate at 15.46 min (A) at 400nm (B).

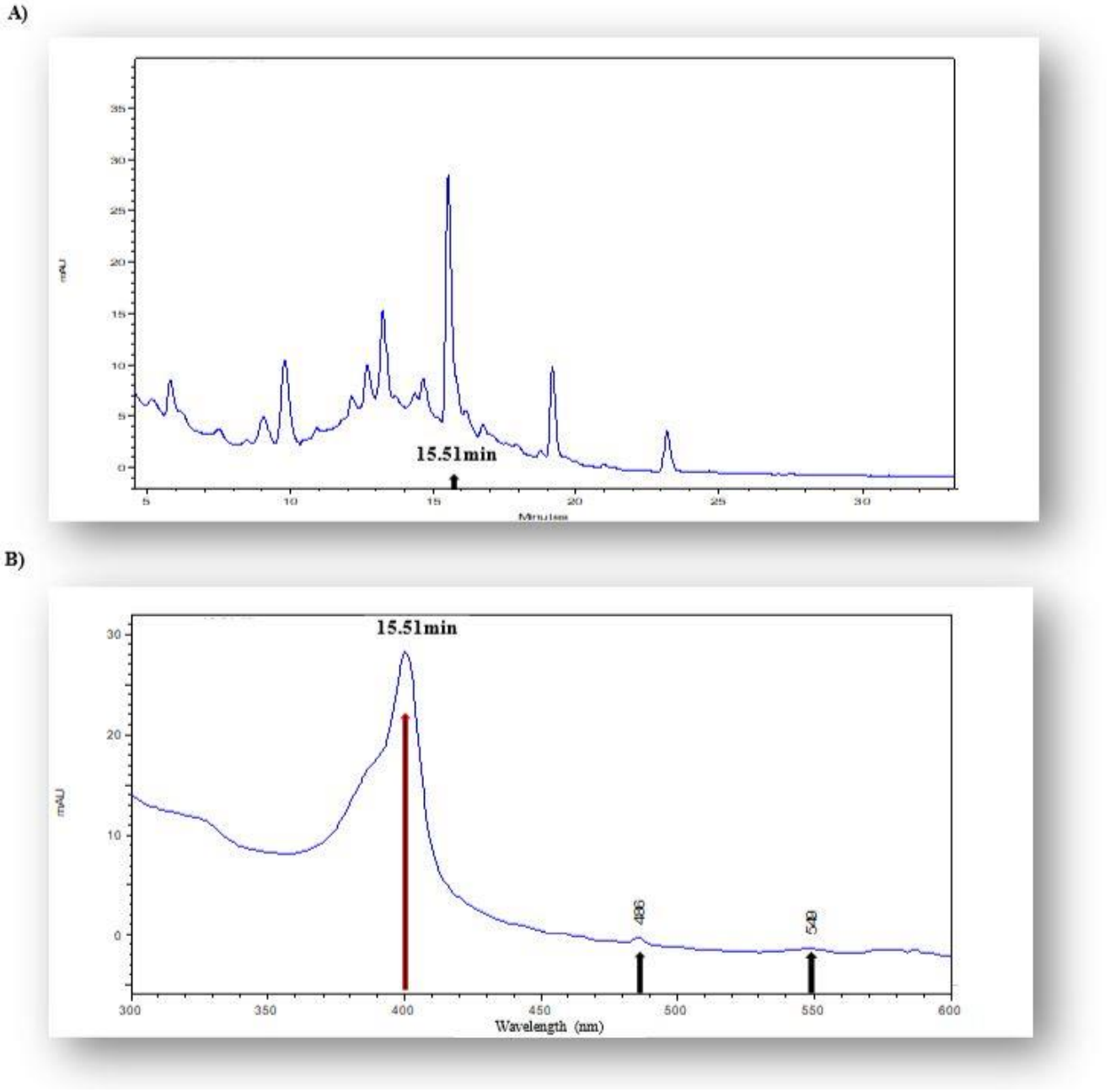

Figure 3.11 – Analysis of the *E. coli* Δ*cgdH*_pØ strain with the ethyl-acetate and acetic acid treatment. Absorption spectra for Δ*cgdH*_pØ strain of the eluate at 15.51 min (A) at 400nm (B).

Comparing the wt and the *E. coli cgdH* mutant strains treated by this ethyl-acetate and acetic acid method, the results are similar (Figure 3.10 and 3.11). The mutant strain does not show more coproporphyrin III than the wt.

The cell extract from the wt strain, obtained by the hydrochloride acid method (Figure 3.12) shows a small peak appears in 3.12A) at a retention time of 15.30 min, at 400nm, corresponding to coproporphyrin III. The *E. coli cgdH* mutant, treated with the same method (Figure 3.13) shows also a small peak with a retention time of 15.32 minutes at 400nm, that resembles coproporphyrin III profile.

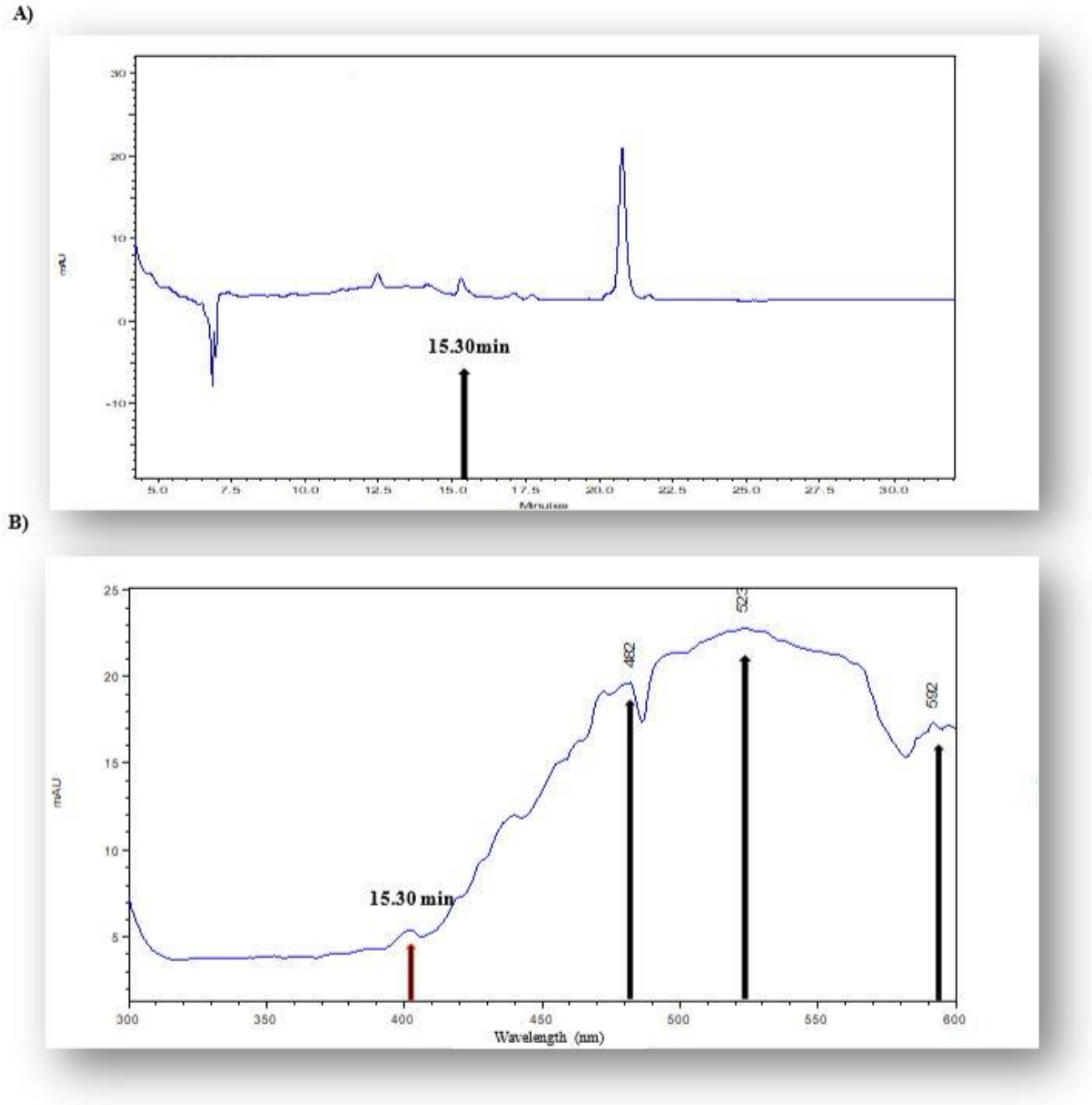

Figure 3.12 - Analysis of the *E. coli* wt strain elution with hydrochloride acid treatment. Absorption spectra for *E. coli* wt strain eluated at 15.30 min (A) at 400nm (B).

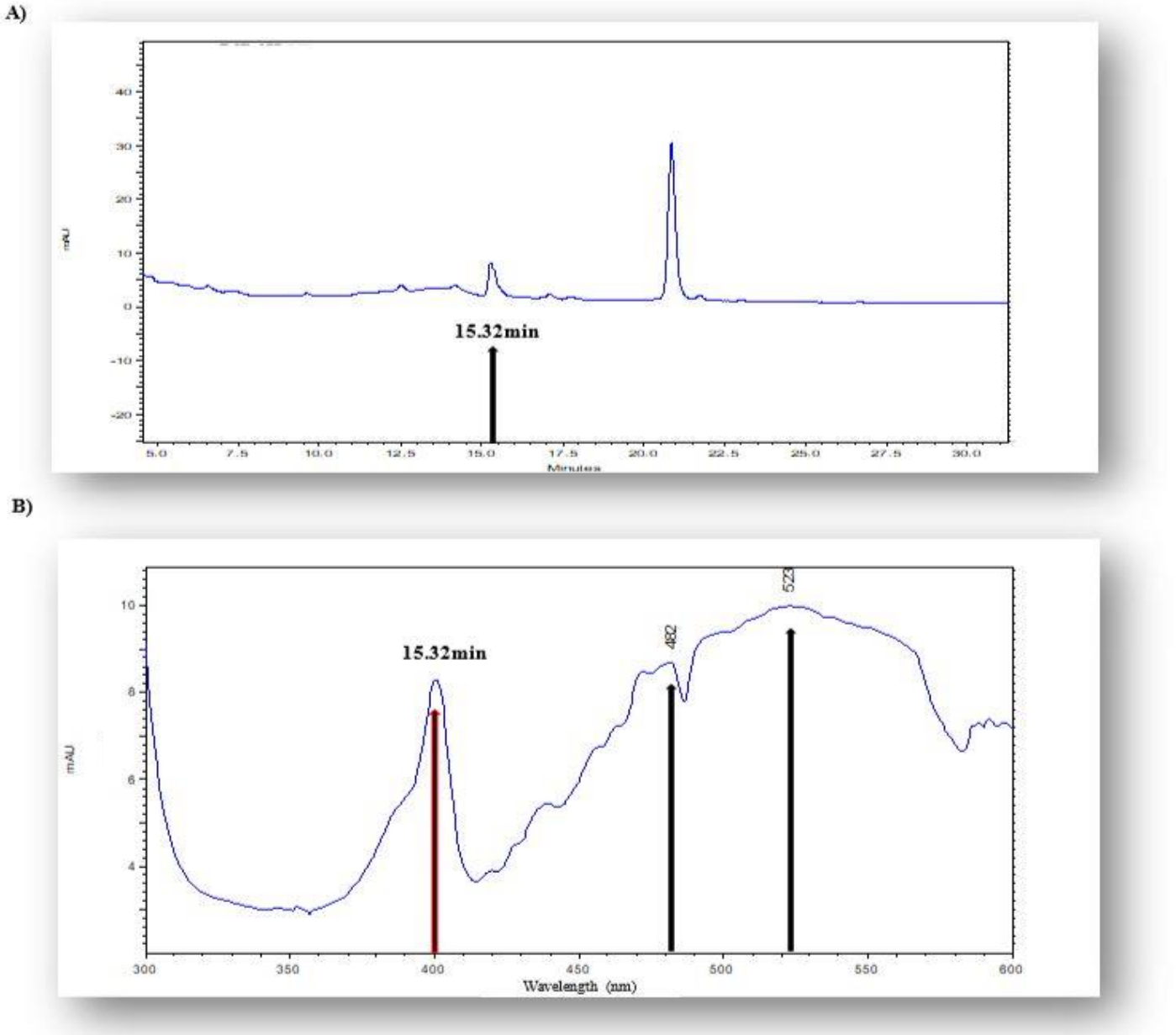

Figure 3.13 - Analysis of the Δ*cgdH*_pØ strain with the hydrochloride acid treatment. HPLC spectrum showed a small peak at 15.32 min (A). Absorption spectrrum of the sample eluted at 15.32 min at 400nm (B).

In the hydrochloride acid method, the *E. coli* wt and the mutant strains show similar retention times at 400nm, that corresponds to the coproporphyrin III but the compound seems to be in a smaller concentration (Figure 3.12 and 3.13). It is notable that another compound is accumulating in higher concentration than coproporphyrin III in both strains, with a peak at an elution time between 20.0-22.5 minutes at the same wavelength (400nm) (Figure 3.12A and 3.13A). This peak may be due to the protohaem formation that is usually detected close to this elution time. This formation could possibly explain the small concentration of coproporphyrin III that is being consumed to form the haem molecule.

A coproporphyrin III accumulation seems to be detected by the ethyl-acetate and acetic acid treatment. This extraction method seems to be more specific to extract coproporphyrin III, than the extraction method based in HCl treatment, where other porphyrins were observe as well.

The retention time of coproprophyrin III standard was of 16.11 minutes. However, the peaks observed in the cell extracts were not exactly at the same time, but close to it (15.46 minutes for wt and 15.51 for the mutant). When compared to the control value, the difference was not high and it can be explained by a variety of reasons, i.e. the control sample was in a pure solution whereas in the cell extracts are not pure solutions and therefore an associated standard error must be considered.

Overall, the results obtained by the porphyrin detection method do not vary between the *E. coli* wt and the mutant. The *cgdH* mutant strain has a similar content of coproporphyrin III when compared with the parental strain, in both methods. Even so, the sample concentration used for this assay may have affected the results since the OD_{600}/mL of the wt strain was more concentrated than the mutant strain.

To conclude, no significant accumulation of coproporphyrin III was observed in *E. coli* Δ*cgdH* which impaired its use to assesse the role of *C.jejuni* CgdH.

Hence, other experiments will be necessary to test to the impact of this gene in the bacterial growth, e.g. the study of the chemical enzymatic activity of $CgdH_{C.jejuni}$, would be interesting to test the activity of this protein *in vitro*.

4

Conclusion and Future Perspectives

Campylobacter jejuni is one of the most common foodborne pathogens worldwide. However, the infection biology of this pathogen remains unclear. Therefore, there is still a wide work to develop in this field and it is essential to continue exploring the molecular mechanisms essential to survive in the host environment.

The importance of haem biosynthesis in the development of *C. jejuni* remains still to be elucidated, but haem homeostasis is known to be a key factor for bacterial development and host pathogens' survival. This work was focused on deciphering the haem biosynthetic pathway of *C. jejuni*. It was shown that *C. jejuni* possesses a PPD pathway encoding for active and functional UroD and PpfC enzymes. However, determination of the activity of CgdH, an intermediate enzyme of the pathway, was unsuccessful due to the scarce work in this type of enzymes in the bibliography.

Further studies should aim the understanding of the physiological relevance of haem biosynthesis in *C. jejuni*. Different work might be done namely protein-protein interactions studies in a two-hybrid system analysis of the expression patterns of the haem biosynthetic genes during stress or determination of the effect of *C. jejuni* mutants during infection of eukaryotic cells.

5

References

Allos, B. M. (2001). Campylobacter jejuni Infections : Update on Emerging Issues and Trends. *Clinical Infectious Diseases*, *32*(8), 1201–1206.

Altekruse, S. F., Stern, N. J., Fields, P. I., Swerdlow, D. L., Food, U. S., & Administration, D. (1999). Campylobacter jejuni — An Emerging Foodborne Pathogen. *Emerging Infectious Diseases*, *5*(1), 28–35.

Ang, C. W. (2001). Guillain-Barré Syndrome- and Miller Fisher Syndrome-Associated Campylobacter jejuni Lipopolysaccharides Induce Anti-GM 1 and Anti-GQ 1b Antibodies in Rabbits. *Infection and Immunity*, *69*(4), 2462–2469.

Bali, S., Lawrence, A. D., Lobo, S. A., Saraiva, L. M., Golding, B. T., Palmer, D. J., … Warren, M. J. (2011). Molecular hijacking of siroheme for the synthesis of heme and d 1 heme. *PNAS*, *108*(45), 18260–18265.

Bolton, D. J. (2015). Campylobacter virulence and survival factors. *Food Microbiology*, *48*, 99–108.

Celis, A. I., & Dubois, J. L. (2019). Making and breaking heme. *Current Opinion in Structural Biology*, *59*, 19–28.

Center, C. G. S. (2006). Coli Genetic Stock Center. Retrieved December 2, 2020, from https://cgsc.biology.yale.edu/KeioList.php

Dailey, H. A., Dailey, T. A., Gerdes, S., Jahn, D., Jahn, M., Brian, M. R. O., & Warren, J. (2017). Prokaryotic Heme Biosynthesis : Multiple Pathways to a Common Essential Product. *Microbiology and Molecular Biology Reviews*, *81*(1).

Duncan, M., & Horan, N. (2003). Microbial nutrition and basic metabolism. In M. Duncan & N. Horan (Eds.), *The Handbook of Water and wastewater microbiology* (1st ed., pp. 3–5). Elsevier Science Publishing Co INC International Concepts.

Giustarini, D., Rossi, R., Milzani, A., & Dalle-Donne, I. (2008). Nitrite and Nitrate Measurement by Griess Reagent in Human Plasma: Evaluation of Interferences and Standardization. In *Methods in enzymology* (pp. 364–365). Elsevier Ltd.

Inoue, H., Nojima, H., & Okayama, H. (1990). High efficiency transformation of E s c h e r i c h i a coli with plasmids. *Gene*, *96*(1), 23–28.

Ji, X., Mo, T., Liu, W., Ding, W., Deng, Z., & Zhang, Q. (2019). Revisiting the Mechanism of the Anaerobic Coproporphyrinogen III Oxidase HemN. *Angewandte Chemie*, *131*(19), 6301–6304.

Layer, G., Reichelt, J., Jahn, D., & Heinz, D. W. (2010). Structure and function of enzymes in heme biosynthesis. *Protein Science : A Publication of the Protein Society*, *19*(6), 1137–1161.

Lobo, S. A. L., Lawrence, A. D., Romão, C. V, Warren, M. J., Teixeira, M., & Saraiva, L. M. (2014). Characterisation of Desulfovibrio vulgaris haem b synthase , a radical SAM family member. *BBA - Proteins and Proteomics*, *1844*(7), 1238–1247.

Lobo, S. A. L., Scott, A., Videira, M. A. M., Winpenny, D., Gardner, M., Palmer, M. J., … Saraiva, L. M. (2015). Staphylococcus aureus haem biosynthesis : characterisation of the enzymes involved in final steps of the pathway. *Molecular Microbiology*, *97*(3), 472–487.

Mancini, S., & Imlay, J. A. (2015). The induction of two biosynthetic enzymes helps Escherichia coli sustain heme synthesis and activate catalase during hydrogen peroxide stress. *Molecular Microbiology*, *96*(4), 744–763.

NAKAHIGASHI, K., NISHIMURA, K., MIYAMOTO, K., & INOKUCHI, H. (1991). Photosensitivity of a protoporphyrin-accumulating , light-sensitive mutant (visA) of Escherichia coli K-12. *PNAS*, *88*(23), 10520–10524.

National Institute of Genetics, Microbial Physiology Laboratory, N. E. coli. (2012). NBPR E.coli Strain. Retrieved December 2, 2020, from https://shigen.nig.ac.jp/ecoli/strain/resource/strainGeneMutant/list/IH_ECOLI_MUTANT_COLLECTION

Panek, H., & Brian, M. R. O. (2002). A whole genome view of prokaryotic haem biosynthesis. *Microbiology (Reading, England)*, *148*(8), 2273–2282.

Parkhill, J., Wren, B. W., Mungall, K., Ketley, J. M., & Churcher, C. (2000). The genome sequence of the food-borne pathogen Campylobacter jejuni reveals hypervariable sequences. *Nature*, *403*(6770), 665–668.

Pontrelli, S., Chiu, T., Lan, E. I., Chen, F. Y., Chang, P., & Liao, J. C. (2018). Escherichia coli as a host for metabolic engineering. *Metabolic Engineering*, *50*, 16–46.

Purdy, D., Buswell, C. M., Hodgson, A. E., Mcalpine, K., Henderson, I., & Leach, S. A. (2000). Characterisation of cytolethal distending toxin (CDT) mutants of Campylobacter jejuni. *J Med Microbiol.*, *49*, 473–479.

Ridley, K. A., Rock, J. D., Li, Y., & Ketley, J. M. (2006). Heme Utilization in Campylobacter jejuni □. *JOURNAL OF BACTERIOLOGY*, *188*(22), 7862–7875.

Sarvan, S., Yeung, A., & Stintzi, A. (2019). Purification and characterization of Campylobacter jejuni ferric uptake regulator. *Biometals*, *32*(3), 491–500.

Sasarman, A., Chartrand, P., Lavoie, M., Tardif, D., Poschek, R., & Lapointe, C. (1979). Mapping of a New hem Gene in Escherichia coli K12. *Journal of General Microbiology*, *113*(2), 297–303.

Sasarman, A., Chartrand, P., Proschek, R., Desrochers, M., Tardif, D., & Lapointe, C. (1975). Uroporphyrin-Accumulating Mutant of Escherichia coli K-12. *Journal of Bacteriology*, *124*(3), 1205–1212.

Stroupe, M. E., Leech, H. K., Daniels, D. S., Warren, M. J., & Getzoff, E. D. (2003). CysG structure reveals tetrapyrrole-binding features and novel regulation of siroheme biosynthesis. *Nature Structural Biology*, *10*(12), 1064–1073.

Tripathy, B. C., Sherameti, I., Oelmüller, R., Tripathy, B. C., Sherameti, I., & Oelmüller, R. (2010). Siroheme An essential component for life on earth. *Plant Signaling & Behavior*, *5*(1), 14–20.

Tyson, K., Metheringham, R., Griffiths, L., & Cole, J. (1997). Characterisation of Escherichia coli K-

12 mutants defective in formate-dependent nitrite reduction : essential roles for hemN and the menFDBCE operon. *Arch Microbiol*, *168*(5), 403–411.

Videira, M. A. M., Lobo, S. A. L., Sousa, F. L., & Saraiva, L. M. (2019). Identification of the sirohaem biosynthesis pathway in Staphylococcus aureus. *FEBS*, *287*(8), 1537–1553.

Videira, M., Lobo, S., & Saraiva, L. (2018). Staphylococcus aureus haem biosynthesis and acquisition pathways are linked through haem monooxygenase lsdG. *Molecular Microbiology*, *109*(3), 385–400.

Walker, R. I., Caldwell, M. B., Lee, E. C., Guerry, P., Trevor, J., & Ruiz-palacios, G. M. (1986). Pathophysiology of Campylobacter Enteritis. *Microbiology Reviews*, *50*(1), 81–94.

Wassenaar, T. M. (1997). Toxin Production by Campylobacter spp . *Clinical Microbiology Reviews*, *10*(3), 466–476.

WHO. (2020). World Health Organization. Retrieved November 13, 2020, from https://www.who.int/news-room/fact-sheets/detail/campylobacter

Young, K. T., Davis, L. M., & Dirita, V. J. (2007). Campylobacter jejuni : molecular biology and pathogenesis. *Nat Rev Microbiol* ., *5*(9), 665–679.

Zhang, J., Kang, Z., Chen, J., & Du, G. (2015). Optimization of the heme biosynthesis pathway for the production of 5-aminolevulinic acid in Escherichia coli. *Scientific Reports*, *5*(8584), 1–7.

6

Appendix

Appendix 6.1- Primers for cloning of haem biosynthesis.

Nº	Primer location	Plasmid to insert	Restriction site	Cje Gene	Primer sequence	Tm (ºC)
1	Forward *uroD*	pPR-IBA 2, PUC 18	KpnI	*uroD*	GGCCGGTACCCATGATTTTTATCGATGCTTGC	53.5
2	Reverse *uroD*	pPR-IBA 2,pPR-IBA 1, PUC 18	AvrII, BamHI	*uroD*	CCGGGGATCCTTAACCTAGGTCATTTAGCTGAACTTTCTT	53.5
3	Forward *uroD*	pPR-IBA 1	KpnI	*uroD*	GGCCGGTACCATGATTTTTATCGATGCTTGC	53.5
4	Forward $cgdH_1$	pPR-IBA 2, PUC 18	EcoRI	$cgdH_1$	CCGGGAATTCGATGAGAGATTATAAAGCTTT	55.1
5	Reverse $cgdH_1$	pPR-IBA 2,pPR-IBA 1, PUC 18	AvrII, BamHI	$cgdH_1$	CCGGGGATCCTAACCTAGGTTACACCGTTTTTGAGAATA	55.1
6	Forward $cgdH_1$	pPR-IBA 1	EcoRI	$cgdH_1$	CCGGGAATTCATGAGAGATTATAAAGCTTT	55.1
7	Forward $pgdH_2$	pPR-IBA 2, PUC 18	EcoRI	$pgdH_2$	CCGGGAATTCGATGACAGAATGGATTAATGA	55
8	Reverse $pgdH_2$	pPR-IBA 2,pPR-IBA 1, PUC 18	AvrII, BamHI	$pgdH_2$	CCGGGGATCCTAACCTAGGCTAAAAGGGACGAACAACCA	55
9	Forward $pgdH_2$	pPR-IBA 1	EcoRI	$pgdH_2$	CCGGGAATTCATGACAGAATGGATTAATGA	55
10	Forward *ppfC*	pPR-IBA 2, PUC 18	EcoRI	*ppfC*	CCGGGAATTCGGTGAAATTAGTTTTATTTTT	55.1
11	Reverse *ppfC*	pPR-IBA 2,pPR-IBA 1, PUC 18	AvrII, BamHI	*ppfC*	CCGGGGATCCTAACCTAGGTTAGTTAAGATCAGATAAAT	55.1
12	Forward *ppfC*	pPR-IBA 1	EcoRI	*ppfC*	CCGGGAATTCGTGAAATTAGTTTTATTTTT	55.1